

Periodic Solutions of a System of Complex ODEs. II. Higher Periods

F. CALOGERO^{y,z} and M. SOMMACAL^z

^y Dipartimento di Fisica, Università di Roma "La Sapienza", 00185 Roma, Italy

^z Istituto Nazionale di Fisica Nucleare, Sezione di Roma, Italy

E-mail: francesco.calogero@roma1.infn.it, francesco.calogero@uniroma1.it

E-mail: matteo.sommacal@roma1.infn.it

Received March 4, 2002; Accepted April 5, 2002

Abstract

In a previous paper the real evolution of the system of ODEs

$$\begin{aligned} \dot{z}_n + z_n &= \sum_{m=1; m \neq n}^N g_{nm} (z_n - z_m)^3; \\ z_n &= z_n(t); \quad \dot{z}_n = \frac{dz_n(t)}{dt}; \quad n = 1; \dots; N \end{aligned}$$

is discussed in C_N , namely the N -dependent variables z_n , as well as the $N(N-1)$ (arbitrary!) "coupling constants" g_{nm} , are considered to be complex numbers, while the independent variable t ("time") is real. In that context it was proven that there exists, in the phase space of the initial data $z_n(0)$, $\dot{z}_n(0)$, an open domain having finite measure, such that all trajectories emerging from it are completely periodic with period 2, $z_n(t+2) = z_n(t)$. In this paper we investigate, both by analytical techniques and via the display of numerical simulations, the remaining solutions, and in particular we show that there exist many "emerging out of sets of initial data having nonvanishing measures in the phase space of such data" that are also completely periodic but with periods which are integer multiples of 2. We also elucidate the mechanism that yields nonperiodic solutions, including those characterized by a "chaotic" behavior, namely those associated, in the context of the initial-value problem, with a sensitive dependence on the initial data.

1 Introduction

In a previous paper [1] one of us (FC) analyzed, in the complex domain, the dynamical system characterized by the Newtonian equations of motion

$$\begin{aligned} \dot{z}_n + z_n &= \sum_{m=1; m \neq n}^N g_{nm} (z_n - z_m)^3; \\ z_n &= z_n(t); \quad \dot{z}_n = \frac{dz_n(t)}{dt}; \quad n = 1; \dots; N \end{aligned} \tag{1.1}$$

which obtain in the standard manner from the Hamiltonian

$$H(\underline{z}; \underline{p}) = \frac{1}{2} \sum_{n=1}^N p_n^2 + z_n^2 + \frac{1}{4} \sum_{n \neq m=1; n \neq m}^N g_{nm} (z_n - z_m)^2; \quad (1.2a)$$

provided (as we hereafter assume) — even though the main result of [1] holds without this restriction)

$$g_{nm} = g_{mn}; \quad (1.2b)$$

Here and below N is an arbitrary positive integer ($N \geq 2$), the indices n, m run from 1 to N unless otherwise indicated, underlined quantities are N -vectors, say $\underline{z} = (z_1; \dots; z_N)$, and all quantities (namely, the N "canonical coordinates" z_n , the N "canonical momenta" p_n , the $N(N-1)/2$ "coupling constants" g_{nm}) are complex, while the independent variable t ("time") is instead real. Of course the N complex equations of motion (1.1) can be reformulated [1] as $2N$ real — and as well Hamiltonian [2] — equations of motion, by introducing the real and imaginary parts of the coordinates z_n , $z_n = x_n + iy_n$, or their amplitudes and phases, $z_n = r_n \exp(i\varphi_n)$:

$$\begin{aligned} \dot{x}_n + x_n &= \sum_{m=1; m \neq n}^N r_{nm}^6 a_{nm} x_{nm} x_{nm}^2 - 3y_{nm}^2 - b_{nm} y_{nm} y_{nm}^2 - 3x_{nm}^2 \\ &= \sum_{m=1; m \neq n}^N r_{nm}^3 \dot{\varphi}_{nm} j \cos(\varphi_{nm} - \varphi_{nm}); \end{aligned} \quad (1.3a)$$

$$\begin{aligned} \dot{y}_n + y_n &= \sum_{m=1; m \neq n}^N r_{nm}^6 a_{nm} y_{nm} y_{nm}^2 - 3x_{nm}^2 - b_{nm} y_{nm} x_{nm}^2 - 3y_{nm}^2 \\ &= \sum_{m=1; m \neq n}^N r_{nm}^3 \dot{\varphi}_{nm} j \sin(\varphi_{nm} - \varphi_{nm}); \end{aligned} \quad (1.3b)$$

where of course

$$\begin{aligned} z_n &= x_n + iy_n; \\ z_{nm} - z_n - z_m &= x_n - x_m + i(y_n - y_m) = x_{nm} + iy_{nm} = r_{nm} \exp(i\varphi_{nm}); \\ g_{nm} &= a_{nm} + ib_{nm} = \dot{\varphi}_{nm} j \exp(i\varphi_{nm}); \end{aligned} \quad (1.3c)$$

We shall return to the motivations for this choice to investigate the system (1.1) in the complex domain at the end of this Section 1.

If all the coupling constants coincide, $g_{nm} = g$, the Hamiltonian system (1.1) is a well-known completely integrable many-body model (see for instance [2] and the references quoted there), and all its nonsingular solutions are completely periodic with period 2π , or possibly an integer multiple of 2π . (Indeed, in this integrable case the N coordinates $z_n(t)$ can be identified with the N zeros of a polynomial of degree N the coefficients of which are periodic in t with period 2π , so that the set of these N zeros is also periodic with period 2π , and each individual zero is therefore also periodic, although possibly with a larger period which is an integer multiple of 2π due to a possible reshuffling of the zeros as the motion

unfolds; in the real case with all coupling constants equal and positive, $g_{nm} = g > 0$, when the motions are confined to the real axis and no such reshuffling can occur due to the singular and repulsive character of the two-body forces, all real solutions are nonsingular and completely periodic with period 2, $\underline{z}(t+2) = \underline{z}(t)$; see for instance [2]). Here we focus instead on the more general case with completely arbitrary coupling constants g_{nm} , which is generally believed not to be integrable. But even in this case—as proven in [1]—there does exist a domain of initial data $\underline{z}(0)$, $\dot{\underline{z}}(0)$ having in finite measure in phase space—indeed, having a measure which is a finite fraction of that of the entire phase space—such that all the trajectories originating from it are completely periodic with period 2, $\underline{z}(t+2) = \underline{z}(t)$. As pointed out in [1], this is a somewhat surprising finding, inasmuch as it negates the expectation that, for a nonlinear dynamical system with several degrees of freedom that possesses completely periodic trajectories emerging from some specific initial data, any generic variation of these initial data destroy the complete periodicity of the trajectories or at least change their period—unless the system is essentially equivalent (say, via an appropriate change of variables) to a linear system (such as (1.1) with all coupling constants vanishing, $g_{nm} = 0$), which is certainly not the case for the system (1.1) with arbitrary coupling constants g_{nm} , at least not in any manner explicitly computable in closed form.

But, as shown in [1], this fact is a rather elementary consequence of an approach (a “trick”) introduced and rather extensively used recently to evince analogous results (see [2] and the references quoted there, as well as [3, 4, 5]). This same trick can as well be exploited to investigate the remaining solutions, namely those not belonging to the class of completely periodic solutions with period 2—the existence of which was proven in [1]. This we do in the present paper, and we also confirm the insight thereby gained by exhibiting numerical solutions of (1.1) performed via a computer code created by one of us (MS) [6]. In particular we demonstrate below the existence of open domains of initial data, having nonvanishing measures in the phase space of such data, which also yield completely periodic solutions, but with periods which are integer multiples of 2, and we also elucidate the mechanism that originates non-periodic and chaotic solutions.

In the next Section (the first part of which is closely patterned after Section 2 of [1] and is reported here to make this paper self-contained) the “trick” mentioned above—which in fact amounts to a change of (dependent and independent) variables—is introduced. In Section 3 the analyticity properties in a time-like complex variable are investigated of the solutions of the system of ODEs, see (2.5), related to (1.1) via the trick. The implications of these findings as regards the periodicity of certain solutions of (1.1) are discussed in Section 4; in particular the mechanism that underlies the existence of completely periodic motions with higher periods (integer multiples of 2), and of non-periodic and chaotic motions, is elucidated. In Section 5 numerical examples of these trajectories are exhibited. In Section 6 some final remarks are proffered. Two appendices complete our presentation: Appendix A contains some developments (confined there not to interrupt the flow of presentation in Section 3) concerning the analytic structure of the solutions of the evolution equations (2.5); Appendix B focuses on the three-body case ($N = 3$), in particular it reports its reducibility to quadratures and a discussion of the information about the analytic behavior of the solutions of (2.5) entailed by this fact.

Let us end this introductory Section 1 with some remarks on the choice to investigate the motion determined by the Newtonian equations (1.1) in the complex, rather than the

real, domain. A clear hint that, at least from a mathematical point of view, this is a more natural environment to work in, comes already from the treatment of (1.1) in the integrable case with equal coupling constants, $g_{nm} = g$, since, as mentioned above, it is then appropriate to identify the N particle positions $z_n = z_n(t)$ with the N zeros of a time dependent (monic) polynomial of degree N in z , say $P_N(z; t)$ such that $P_N[t; z_n(t)] = 0$ (see for instance Ref. [2]); and clearly the natural environment to investigate the zeros of a polynomial is the complex plane rather than the real line. In our context, an essential motivation to work in the complex comes from the important role that analyticity properties play in our treatment, see below. Moreover motions roaming over the complex plane display a much richer dynamics than those restricted to the real line, especially in the case with singular interparticle forces, because of the possibility in the former case, but not in the latter, that particles go around each other. And it is then natural to re-interpret the (complex) N -body problem (1.1) as describing the (real) motion of N particles (in the plane), by introducing a one-to-one correspondence among the complex coordinates $z_n = x_n + iy_n$, see (1.3c), and the real two-vectors in the plane $\mathbf{r}_n = (x_n; y_n)$. But this approach, that is quite convenient to identify interesting many-body problems in the plane (see Chapter 4 of Ref. [2]), suffers in the present case from a drawback: the resulting many-body problem in the plane is not rotation-invariant, see (1.3). Indeed the many-body problem (1.3) is characterized by a (clearly rotation-invariant) harmonic-oscillator one-body force attracting every particle towards the origin, and by a (clearly not rotation-invariant) singular two-body force acting among each particle pair. As clearly seen from (1.3), the strength of the two-body force is proportional to the inverse cube of the (Euclidian) interparticle distance, hence it generally diverges when two particles collide; but this force also depends, both in modulus and direction, from the orientation of the interparticle vector, as well as from the phase φ_{nm} of the relevant interparticle coupling constant (1.3c). Indeed the two-body force \mathbf{f}_{nm} acting on the n -th particle due to the m -th particle is the two-vector $\mathbf{f}_{nm} = r_{nm}^{-3} \mathbf{g}_{nm} j(\cos(\varphi_{nm} - 3\varphi_{nm}); \sin(\varphi_{nm} - 3\varphi_{nm}))$, which is generally not aligned to the interparticle distance $\mathbf{r}_{nm} = r_{nm}(\cos \varphi_{nm}; \sin \varphi_{nm})$, see (1.3). The diligent reader is advised to try and become familiar with the specific implications of this fact, as they will be eventually helpful to understand the trajectories of the solutions of the model (1.1), see Section 5.

2 The trick

In this section we describe the "trick" [14] that underlies our subsequent findings, and at the end we mention a remarkable property of the system of ODEs (1.1). But firstly we rewrite, mainly for notational convenience, these equations of motion, (1.1), as follows:

$$\ddot{z}_n + \sum_{m=1; m \neq n}^N g_{nm} (z_n - z_m)^{-3}; \quad (2.1a)$$

and we note that the corresponding Hamiltonian reads

$$H(\underline{z}; \underline{p}) = \frac{1}{2} \sum_{n=1}^N p_n^2 + \frac{1}{4} \sum_{n, m=1; n \neq m}^N g_{nm} (z_n - z_m)^{-2}; \quad (2.1b)$$

Here we introduce the additional constant ω , which is hereafter assumed to be positive, $\omega > 0$, and to which we associate the basic period

$$T = 2/\omega : \quad (2.2)$$

In the following it will sometimes be convenient to set $\omega = 1$ so that (2.1a) coincide with (1.1) and the basic period becomes $T = 2$, or to set instead $\omega = 2$ so that the basic period becomes unity, $T = 1$. Of course these cases are all related via a rescaling of the dependent and independent variables, since clearly by setting

$$z(t) = az(\tau); \quad \tau = bt; \quad \omega = \omega_0 b; \quad g_{nm} = a^2 b^2 g_{nm} \quad (2.3a)$$

with a, b two positive rescaling constants which can be chosen at our convenience, the ODEs (2.1a) get reformulated in a completely analogous "tilded" version,

$$z_n^{(0)} + \omega_0^2 z_n = \sum_{m=1; m \neq n}^N g_{nm} (z_n - z_m)^3; \quad (2.3b)$$

where of course here the primes indicate differentiations with respect to the argument of the function they are appended to, $z^{(0)} = dz(\tau)/d\tau$. Note in particular that by setting $b = a^2 = \omega_0$ one gets $\omega = 1$, $g_{nm} = g_{nm}$, namely the tilded version (2.3b) reproduces essentially (1.1).

Now, the "trick". Let us set

$$z_n(t) = \exp(-i\omega_0 t) \tilde{z}_n(t); \quad (2.4a)$$

$$\tilde{z}_n(t) = [\exp(2i\omega_0 t) - 1] \tilde{z}_n(t); \quad (2.4b)$$

As can be readily verified, this change of (dependent and independent) variables, (2.4), transforms (2.1a) into

$$\tilde{z}_n^{(0)} = \sum_{m=1; m \neq n}^N g_{nm} (\tilde{z}_n - \tilde{z}_m)^3; \quad (2.5)$$

Here and below appended primes denote derivatives with respect to the new independent variable τ , while of course the dots in (2.1a) and below denote as usual derivatives with respect to the real time t .

The change of variables (2.4) entails the following relations among the initial data, $z(0)$, $\dot{z}(0)$, respectively $\tilde{z}(0)$, $\tilde{z}^{(0)}(0)$, for (2.1a) respectively (2.5):

$$z_n(0) = \tilde{z}_n(0); \quad (2.6a)$$

$$\dot{z}_n(0) = \tilde{z}_n^{(0)}(0) - i\omega_0 \tilde{z}_n(0); \quad (2.6b)$$

We now observe that, as the (real, "physical time") variable t varies from 0 to $T = 2/\omega_0 = 2/\omega$, the (complex) variable z travels (counterclockwise) full circle over the circular contour C , the diameter of which, of length $1/\omega_0 = T/2$, lies on the upper-half of the complex z -plane, with its lower end at the origin, $\omega_0 = 0$, and its upper end at $\omega_0 = i\omega_0$. Hence if the solution $\tilde{z}(\tau)$ of (2.5) which emerges from some assigned initial data $\tilde{z}(0)$, $\tilde{z}^{(0)}(0)$

is holomorphic, as a (N -vector-valued) function of the complex variable z , in the closed circular disk C encircled by the circle C^* in the complex z -plane, then the corresponding solution $\underline{z}(t)$ of (2.1a), related to $\underline{z}(z)$ by (2.4), is completely periodic in t with period T , $\underline{z}(t+T) = \underline{z}(t)$ (see (2.2); and note that $\underline{z}(z)$, considered as function of the real variable t , is then periodic with period $T=2$, but $\underline{z}(t)$ is instead antiperiodic with period $T=2$, $\underline{z}(t+T=2) = -\underline{z}(t)$, due to the prefactor $\exp(-i!t)$, see (2.4a)).

In [1] it was proven that there indeed exists a domain, having in finite measure in phase space, of initial data $\underline{z}(0), \dot{\underline{z}}(0)$ such that the corresponding solutions $\underline{z}(z)$ of (2.5) are holomorphic in z in the disk C and this fact implies the existence of an open domain, having as well in finite measure in phase space, of corresponding initial data $\underline{z}(0), \dot{\underline{z}}(0)$ such that the corresponding solutions $\underline{z}(t)$ of (2.1a) are completely periodic with period T , $\underline{z}(t+T) = \underline{z}(t)$. In the following Section 3 we show that the singularities of the solutions $\underline{z}(z)$ of (2.5) considered as functions of the complex variable z are branch points of square-root type, and in Section 4 we infer from this that, whenever the solution $\underline{z}(z)$ of (2.5) has a finite number of such branch points inside the circle C^* generally nested inside each other, namely occurring on different Riemann sheets then the corresponding solution $\underline{z}(t)$ of (2.1a), considered as a function of the real "time" variable t , is again completely periodic, albeit now with a period which is an integer multiple of T . We also infer that when instead the solution $\underline{z}(z)$ of (2.5) has an infinite number of such square-root branch points inside the circle C^* again, generally nested inside each other, namely occurring on different Riemann sheets then the corresponding solution $\underline{z}(t)$ of (2.1a), considered again as a function of the real "time" variable t , may be not periodic at all indeed it generally behaves chaotically (actually, strictly speaking, the chaotic character is not a property of a single solution, it rather has to do with the difference among the long-time behavior of a solution and those of other solutions which emerge from almost identical initial data see below).

Finally let us report a remarkable property of the system of ODEs (2.1a). First of all we recall a trivial result, namely that the center of mass of the system (2.1a),

$$\underline{z}(t) = N^{-1} \sum_{n=1}^N \underline{z}_n(t); \quad (2.7a)$$

rotates uniformly with period T , see (2.2), since clearly these equations of motion, (2.1a), entail

$$\underline{z} + !^2 \underline{z} = 0; \quad (2.7b)$$

hence

$$\underline{z}(t) = \underline{z}(0) \cos(!t) + \underline{z}(0) (!)^{-1} \sin(!t); \quad (2.7c)$$

A less trivial result is that the sum of the squares of the particle coordinates,

$$z^{(2)}(t) = N^{-1} \sum_{n=1}^N [\underline{z}_n(t)]^2; \quad (2.8a)$$

evolves as well periodically, with period $T=2$. Indeed, as shown below, the equations of motion (2.1a) entail

$$z^{(2)} + (2!)^2 z^{(2)} = (4=N)H; \quad (2.8b)$$

where the Hamiltonian H , see (2.1b), is of course a constant of motion. Hence

$$z^{(2)}(t) = a \exp(2i!t) + b + c \exp(-2i!t); \quad (2.8c)$$

where the three constants a, b, c are of course related to the initial data as follows:

$$z(0) = a + b + c = N^{-1} \sum_{n=1}^N [z_n(0)]^2; \quad (2.9a)$$

$$z(0) = 2i! (a - b) = (2i!N)^{-1} \sum_{n=1}^N z_n(0) z_n(0); \quad (2.9b)$$

$$z^{(2)}(0) = (2i!)^2 (a + b) = (2i!)^2 z^{(2)}(0) + (4i!N) H; \quad (2.9c)$$

There remains to prove that the equations of motion (2.1a) entail (2.8b). Indeed by differentiating twice the definition (2.8a) one gets

$$z^{(2)} = \frac{2}{N} \sum_{n=1}^N z_n^2 + z_n z_n; \quad (2.10a)$$

and by using the equations of motion (2.1a) this yields

$$z^{(2)} = \frac{2}{N} \sum_{n=1}^N z_n^2 + \sum_{n \neq m=1; m \in N}^N g_{nm} z_n (z_n - z_m)^3; \quad (2.10b)$$

Hence (using again the definition (2.8a), and the symmetry of the coupling constants, see (1.2b))

$$z^{(2)} + 4i!^2 z^{(2)} = \frac{2}{N} \sum_{n=1}^N z_n^2 + \sum_{n \neq m=1; m \in N}^N \frac{1}{2} g_{nm} (z_n - z_m)^2; \quad (2.10c)$$

and using again (1.2b), as well as the Hamiltonian equations $\dot{z}_n = p_n$ entailed by (2.1b), it is immediately seen, via (2.1b), that the right-hand side of (2.10c) coincides with the right-hand side of (2.8b). But the left-hand sides obviously coincide as well, so the result is proven. (We provided here a proof of this result for completeness, although of course this result can as well be directly inferred via the trick from the analogous finding recently proved for the system (2.5) [7]).

3 The analytic structure of the solutions of (2.5)

In this section we discuss the analytic structure of the solutions $z_n(t)$ of the system of ODEs (2.5), considered as functions of the complex variable t , and in particular we show that the singularities of these functions are branch points of square-root type (see below).

These singularities are of course associated with values of the dependent variables z_n that cause the right-hand side of (2.5) to diverge, namely they are associated with "collisions" of two or more of the coordinates z_n . (By definition the "collision" of two or more

coordinates occurs when their values coincide; but we use inverted commas to underline that, since we are considering complex values of the independent variable τ , such "collisions" need not correspond to actual collisions of the "particles" the motion of which as the real "time" variable t unfolds is described by the "physical" equations of motion (1.1) or (2.1a) — we shall return to this point below). Clearly the generic case corresponds to two-body collisions, occurring at some value $\tau = \tau_b$ such that, say,

$$x_1(\tau_b) = x_2(\tau_b); \quad (3.1a)$$

Here and below, without loss of generality, when discussing two-body collisions, we focus on the two particles carrying the labels 1 and 2. Note that it is natural to expect that this equation, (3.1a), have one or more (possibly an infinity) of solutions τ_b in the complex τ -plane for any generic solution $x_i(\tau)$ of the ODEs (2.5); while the equations characterizing a multiple collision, say

$$x_1(\tau_b) = x_2(\tau_b) = x_3(\tau_b) = \dots = x_M(\tau_b); \quad (3.1b)$$

with $2 < M < N$ have generally no solution at all (for a generic solution $x_i(\tau)$ of the ODEs (2.5); there exist of course special solutions of the ODEs (2.5) which feature such multiple collisions, and we discuss them below to demonstrate that they as well feature branch points of square-root type; we moreover believe, due to the scaling character of the equations of motion (2.5), that completely multiple collisions characterized by $M = N$ are, as well as two-body collisions, featured by any generic solution of (2.5) — as suggested by the analysis of the three-body case, see Appendix B).

To demonstrate that the singularity of the solution $x_i(\tau)$ of the ODEs (2.5) associated with the collision (3.1a) is a branch point of square-root type we introduce the following ansatz, valid in the neighborhood of $\tau = \tau_b$:

$$x_1(\tau) = b + v(\tau - \tau_b)^{1/2} + a(\tau - \tau_b)^{3/2} + \sum_{l=4}^{\infty} \frac{X_l^{(1)}}{l!} (\tau - \tau_b)^{l/2}; \quad (3.2a)$$

$$x_2(\tau) = b + v(\tau - \tau_b)^{1/2} + a(\tau - \tau_b)^{3/2} + \sum_{l=4}^{\infty} \frac{X_l^{(2)}}{l!} (\tau - \tau_b)^{l/2}; \quad (3.2b)$$

$$x_n(\tau) = b_n + v_n(\tau - \tau_b)^{1/2} + \sum_{l=4}^{\infty} \frac{X_l^{(n)}}{l!} (\tau - \tau_b)^{l/2}; \quad n = 3, 4, \dots, N; \quad (3.2c)$$

The fact that this ansatz is consistent with the two-body-collision condition (3.1a) is plain. It can moreover be shown (see Appendix A) that this ansatz, (3.2), is compatible with the ODEs (2.5), and moreover that, while the coefficients b and $X_l^{(n)}$ featured by it are uniquely determined by the requirement that (3.2) satisfy (2.5), the remaining coefficients, namely the 4 constants b, v, a and τ_b , see (3.2a), (3.2b), and the $2(N-2)$ constants b_n, v_n , see (3.2c), are arbitrary (except for the obvious requirements $b_n \neq b, b_n \neq b_m$) — and since altogether the number of these arbitrary constants is $2N$, we infer that this ansatz, (3.2), is adequate to represent in the neighborhood of $\tau = \tau_b$ the general solution of the system of N second-order ODEs (2.5).

We therefore conclude that the singularities associated with the generic solution of (2.1a) are branch points of square-root type, since clearly this is the singularity exhibited

by the right-hand sides of (3.2) | on the assumption that the infinite series they feature do indeed converge in a sufficiently small neighborhood of $\mathbf{z} = \mathbf{z}_b$.

It is easily seen that this same conclusion obtains if consideration is extended to include multiple collisions, see (3.1b). Indeed the corresponding ansatz reads, in analogy to (3.2),

$$\begin{aligned} \mathbf{z}_n(\mathbf{z}) = & \mathbf{b} + \mathbf{z}_n(\mathbf{z}_b)^{1/2} + \mathbf{v}(\mathbf{z}_b) \\ & + a_n(\mathbf{z}_b)^{3/2} + \sum_{l=4}^N \frac{X^l}{l!} \mathbf{z}_n^{(l)}(\mathbf{z}_b)^{1/2}; \quad n = 1; 2; \dots; M; \end{aligned} \quad (3.3a)$$

$$\mathbf{z}_n(\mathbf{z}) = \mathbf{b}_n + \mathbf{v}_n(\mathbf{z}_b) + \sum_{l=4}^N \frac{X^l}{l!} \mathbf{z}_n^{(l)}(\mathbf{z}_b)^{1/2}; \quad n = M+1; M+2; \dots; N; \quad (3.3b)$$

The consistency of this ansatz with the ODEs (2.5) is also demonstrated in Appendix A; but note that, as shown there, only the 3 constants \mathbf{b} , \mathbf{v} , \mathbf{z}_b appearing in the right-hand side of (3.3a), and a common rescaling factor, say a , of the M coefficients a_n , as well as the constants \mathbf{b}_n , \mathbf{v}_n appearing in the right-hand side of (3.3b), are now arbitrary; so, the ansatz (3.3) features altogether $4 + 2(N - M) = 2N - 2(M - 2)$ arbitrary constants. Hence for $M > 2$ this ansatz does not feature the full complement of $2N$ arbitrary constants required in order that (3.3) represent, for \mathbf{z}_b , the general solution of (2.5) | as indeed we expected (since we do not expect the generic solution of (2.5) to feature multiple collisions, at least with $2 < M < N$).

Let us end this section by reporting the similarity solution of (2.5) that indeed features an N -body collision. It reads, as can be easily verified,

$$\mathbf{z}_n(\mathbf{z}) = \mathbf{b} + \mathbf{z}_n(\mathbf{z}_b)^{1/2} + \mathbf{v}(\mathbf{z}_b); \quad (3.4a)$$

with the 3 constants \mathbf{b} , \mathbf{v} and \mathbf{z}_b arbitrary, while the N constants \mathbf{z}_n are instead determined by the N algebraic equations

$$\mathbf{z}_n = \frac{1}{4} \sum_{m=1; m \neq n}^N g_{nm} (\mathbf{z}_n - \mathbf{z}_m)^3; \quad (3.4b)$$

As it is well known (see for instance [2]), in the integrable equal-coupling-constants case,

$$g_{nm} = g; \quad (3.5a)$$

the solution of (3.4b) is

$$\mathbf{z}_n = (\frac{1}{2}g)^{1/4} \mathbf{z}_n; \quad (3.5b)$$

where the N real numbers \mathbf{z}_n are the N zeros of the Hermite polynomial $H_N(\mathbf{z})$ of degree N ,

$$H_N(\mathbf{z}) = 0; \quad (3.5c)$$

Note that the formula (3.5b) defines in fact 4 different sets of coefficients \mathbf{z}_n , due to the 4 possible determinations of the fourth root appearing in the right-hand side of this equation.

Finally let us emphasize that these findings entail that, even in the integrable equal-coupling-constants case, see (3.5a), the solutions of the ODEs (2.5) do not possess the so-called Painlevé property, namely they are not free of movable branch points, indeed their branch points (of square-root type, see for instance the special solution (3.4a)) occur at values $z = z_b$ of the independent variable z which are not a priori predictable, but rather depend, in the context of the initial-value problem, on the initial data. But in the integrable case the number of these branch points is always finite: they are indeed determined by the requirement that the monic polynomial of degree N in the variable, say, z , the N zeros of which are the N coordinates $z_n(z)$ (and the coefficients of which are themselves polynomials of degree N in z), have a double zero (see for instance [2]).

4 Periodicity of the solutions of the system of ODEs (2.1a): theoretical considerations

In this section we analyze the implications of the findings of the previous Section 3 as regards the periodicity of the solutions of the ODEs (2.1a).

We know of course that, if a solution $z_n(z)$ of (2.5) is holomorphic as a function of the complex variable z inside the circle C (see Section 2) and we know that such solutions do exist, in fact in the context of the initial-value problem they emerge out of a set of initial data which has in finite measure in the phase space of such data [1] then the solution $z(t)$ of (2.1a) that corresponds to it via (2.4) is completely periodic with period T , see (2.2),

$$z_n(t+T) = z_n(t): \quad (4.1a)$$

But the transformation (2.4) actually implies, as already noted in Section 2, an additional information, namely that in this case $z(t)$ is completely antiperiodic with period $T=2$,

$$z_n(t+T=2) = -z_n(t): \quad (4.1b)$$

Note that (4.1b) implies (4.1a), while of course (4.1a) does not imply (4.1b).

Let us instead assume that a branch point of a solution $z_n(z)$ of (2.5), occurring, say, at $z = z_b$, does fall inside the circle C in the complex z -plane (see Section 2). Then, due to the square-root nature of this branch point, see (3.2), the evolution of the solution $z_n(z)$ of (2.5) as the real time variable t unfolds is obtained by following the complex time-like variable z as it travels (2.4) along the circular contour C on a two-sheeted Riemann surface. Clearly the change of variable (2.4a), (2.4b) entails then that the corresponding solution $z(t)$ of (2.1a) is just as well completely periodic with period T , see (4.1a), although in this case (4.1b) does no more hold. And of course this conclusion holds provided only one branch point of the solution $z_n(z)$ of (2.5) falls inside the circle C in the main sheet of the Riemann surface associated with this solution, and no other branch point occurs inside the circle C in the second sheet of this Riemann surface, namely on the sheet entered through the cut associated with the branch point occurring inside C on the main sheet of the Riemann surface (of course this Riemann surface might feature many other sheets associated with other branch points occurring elsewhere hence not relevant to our present discussion).

Let us now continue this analysis by considering, more generally, a solution $\underline{z}(t)$ of (2.5) that possibly contains more than one branch point inside the circle C' in the main sheet of its Riemann surface (that do not cancel each other) so that by traveling along the circle C' several additional Riemann sheets are accessed from the main sheet, and let us moreover assume that, on these additional sheets, additional branch points possibly occur inside the circle C' which give access to other sheets, and that possibly on these other sheets there be additional branch points and so on. Let in conclusion B be the total number of additional sheets accessed by a point traveling around and around on the circle C' on the Riemann surface associated with the solution $\underline{z}(t)$ of (2.5). This number B might coincide with the total number of branch points occurring, inside the circle C' , on this Riemann surface or on all its sheets or it might be smaller. Indeed, since each of these branch points is of square-root type, each of the associated cuts if entered into gives access to one additional sheet. But not all these sheets need be accessed; the total number B that are actually accessed depends on the structure of the Riemann surface, for instance no additional sheet at all is accessed if there is no branch point on the main sheet of the Riemann surface even though other branch points may be present inside the circle C' on other sheets of the Riemann surface associated with the solution $\underline{z}(t)$ of (2.5). (It might also be possible that different branch points cancel each other pairwise as is the case for two branch points that are on the same sheet inside the circle C' and generate a cut that starts at one of them and ends at the other). In any case the overall time requested for the point $\underline{z}(t)$ traveling on the Riemann surface to return to its point of departure (say, $\underline{z}(0) = 0$ on the main sheet) is $(B + 1)T = 2$, since a half-period $T = 2$, see (2.4b), is required to complete a tour around the circle C' on each sheet, and the number of sheets to be traveled before getting back to the point of departure is overall $B + 1$ (including the main sheet). Hence in this case, as the real time t evolves, the solution $\underline{z}(t)$ of (2.5) will be completely periodic with period $(B + 1)T = 2$. Hence (see (2.4)) if B is even the corresponding solution $\underline{z}(t)$ of (2.1a) will be completely antiperiodic with the same period $(B + 1)T = 2$, $\underline{z}[t + (B + 1)T] = -\underline{z}(t)$, and completely periodic with the "odd" period $(B + 1)T$, $\underline{z}[t + (B + 1)T] = \underline{z}(t)$. If instead B is odd, the solution $\underline{z}(t)$ of (2.5) as well as the corresponding solution $\underline{z}(t)$ of (2.1a) will both be completely periodic in t with the period $(B + 1)T = 2$ (which might be "even" or "odd" of course, as an integer multiple of the basic period T), $\underline{z}[t + (B + 1)T] = \underline{z}(t)$ (so, in this case, the trajectories of $\underline{z}(t)$ will display no symmetry, in contrast to the previous case).

In this analysis the assumption was implicitly understood that the total number B of additional sheets accessed by traveling around and around on the circle C' on the Riemann surface associated with the solution $\underline{z}(t)$ of (2.5) be finite (a number B which, as we just explained, might coincide with, or be smaller than, the total number of branch points of that Riemann surface that are located inside the circle C' in the complex plane); and moreover we implicitly assumed that no branch point occur exactly on the circle C' . Let us now elaborate on these two points.

If a branch point p_b occurs exactly on the circle C' , then the "physical" equations of motion (2.1a) become singular, due to a particle collision occurring at the real time t_c defined mod $(T = 2)$ (see (2.2)) by the formula

$$p_b = [\exp(2i! t_c) - 1] = (2i!): \quad (4.2)$$

Indeed it is easy to check via (2.4) that the condition that t_c be real coincides with the

requirement that the corresponding value of b , as given by (4.2), fall just on the circular contour C in the complex β -plane. The singularity is of course due to the divergence, at the collision time $t = t_c$, of the right-hand side of the equations of motion (2.1a); there is however no corresponding divergence of the solution $\underline{z}(t)$, which rather has a branch point of square root type at $t = t_c$, see (3.2). But of course this entails that the speeds of the colliding particles diverge at the collision time $t = t_c$ proportionally to $|t - t_c|^{1/2}$, and their accelerations diverge proportionally to $|t - t_c|^{-1/2}$.

There is no a priori guarantee that the number of branch points inside C of a solution $\underline{z}(t)$ of (2.5) be finite, nor that the number B of additional sheets accessed according to the mechanism described above by moving around the circle C on the Riemann surface associated with that solution $\underline{z}(t)$ of (2.5) be finite (of course B might be infinite only if the number of branch points inside C is itself infinite). Obviously in such a case ($B = \infty$), although the complex number $\beta(t)$, (see 2.4b), considered as a function of the real "time" variable t , is still periodic with period $T=2$, neither the solution $\underline{z}(t)$ of (2.5), nor the corresponding solution $\underline{z}(t)$ of (2.1a), will be periodic. The question that might then be raised is whether such a solution — in particular, such a solution $\underline{z}(t)$ of the "physical" Newtonian equations of motion (1.1) corresponding to the many-body problem characterized by the Hamiltonian (1.2) — displays a "chaotic" behavior, namely, in the context of the initial-value problem, a "sensitive dependence" on the initial data. We shall return to this question below.

So far we have discussed the relation among the analytic structure of a solution $\underline{z}(t)$ of (2.5) and the corresponding solution $\underline{z}(t)$ of (2.1a). Let us now return to the simpler cases considered at the very beginning of this analysis and let us consider how the transition from one of the two regimes described there to the other occurs in the context of the initial-value problem for (2.1a), and correspondingly for (2.5), see (2.6). Hence let us assume again that the initial data for (2.1a), and correspondingly for (2.5) (see (2.6)), entail that no branch point of the corresponding solution $\underline{z}(t)$ of (2.5) occurs inside the circular contour C on the main sheet of the associated Riemann surface, so that the corresponding solution $\underline{z}(t)$ of (2.1a) satisfies both (4.1a) and (4.1b). Let us imagine then to modify with continuity the initial data, for instance by letting them depend on an appropriate scaling parameter (a particular way to do so will be introduced in the following Section 5, as a convenient technique to present numerical results). As a consequence the branch points of the solution $\underline{z}(t)$ of (2.5) move, and the Riemann surface associated to this solution $\underline{z}(t)$ of (2.5) gets accordingly modified. We are interested in a movement of the branch points which takes the closest one of them on the main sheet of the Riemann surface from outside to inside the circle C . In the process that branch point will cross the circle C , and the particular set of initial data that correspond to this happening is then just a set of initial data that entails the occurrence of a collision in the time evolution of the many-body problem (2.1a), occurring at a real time $t = t_c$ defined by (4.2), as discussed above. After the branch point has crossed the contour C and has thereby entered inside the circular disk C , the corresponding solution $\underline{z}(t)$ of (2.1a) is again collision-free but its periodicity properties are changed. One might expect that the new solution continue then to satisfy (4.1a) but cease to satisfy (4.1b). This is indeed a possibility, but it is not the only one. Indeed, since the time evolution of the solution $\underline{z}(t)$ of (2.1a) obtains via (2.4) by following the time evolution of the corresponding solution $\underline{z}(t)$ of (2.5) as the point

(t) goes round the circle C^* on the Riemann surface associated with that solution, the occurrence of a branch point inside the circle C^* on the main sheet of that Riemann surface entails that the access is now open to a second sheet, and then possibly to other sheets if, on that second sheet, there also are branch points inside the circle C^* . If this latter possibility does not occur, namely if on that second sheet there are no branch points inside the circle C^* , then indeed there occurs for the corresponding solution $z(t)$ of (2.1a) a transition from a periodicity property characterized by the validity of both (4.1a) and (4.1b), to one characterized by the validity of (4.1a) but not of (4.1b). If instead there is at least one branch point in the second sheet inside the circle C^* , then the periodicity — if any — featured after the transition by the solution $z(t)$ of (2.1a) depends, as discussed above, on the number B of sheets that are sequentially accessed before returning — if ever — to the main sheet.

To simplify our presentation we have discussed above the transition process by taking as point of departure for the analysis the basic periodic solution — that characterized by the validity of both (4.1a) and (4.1b), the existence of which has been demonstrated in [1] — and by discussing how a continuous modification of the initial data may cause a transition to a different regime of periodicity, with the transition occurring in correspondence to the special set of initial data that yields a solution characterized by a particle collision, namely a set of initial data for which the Newtonian equations of motion become singular at a finite real time t_c (defined mod $(T=2)$). But it is clear that exactly the same mechanism accounts for every transition that occurs from a solution $z(t)$ of (2.1a) characterized by a type of periodicity to a solution $z(t)$ of (2.1a) characterized by a different periodicity regime — or by a lack of periodicity.

The final point to be discussed is the question we postponed above, namely the character of the nonperiodic solutions $z(t)$ of (2.1a) (if any), which we now understand to be characterized, in the context of the mechanism described above, by access to an endless sequence of different sheets — all of them generated by branch points of square-root type — of the Riemann surface associated with the corresponding solution $z(t)$ of (2.5). The following two possibilities can be imagined in this connection — which of course does not entail they are indeed both realized.

The first possibility — which we surmise to be the most likely one to be actually realized — is that an infinity of such relevant branch points occur quite closely to the circular contour C^* , hence that there be some of them that occur arbitrarily close to C^* . This then entails that the corresponding nonperiodic solutions $z(t)$ of (2.1a) manifest a sensitive dependence on their initial data (which we consider to be the signature of a chaotic behavior). Indeed a modification, however small, of such initial data entails a modification of the pattern of such branch points, which shall cause some of them to cross over from one to the other side of the circular contour C^* . But then the two solutions $z(t)$ of (2.1a) corresponding to these two assignments of initial data — before and after the modification, however close these data are to each other — will eventually evolve quite differently, since their time evolutions are determined by access to two different sequences of sheets of the Riemann surfaces associated with the two corresponding solutions $z(t)$ of (2.5) — two Riemann surfaces which themselves need not be very different (to the extent one can make such statements when comparing two objects having as complicated a structure as a Riemann surface with an infinite number of sheets produced by an infinite number of branch points of square-root type). So this is the mechanism whereby a chaotic

behavior may develop for the system (1.1) | but of course not in the integrable case with equal coupling constants (in that case, as mentioned above, the number of branch points of the solutions $z(t)$ of (2.5) is always finite, since the N coordinates $z_n(t)$ are in this case the N zeros of a polynomial of degree N the coefficients of which are polynomials in the variable t [2]). Note that the emergence of such a chaotic behavior would not be associated with a local exponential divergence of trajectories in phase space | it would be rather analogous to the mechanism that causes a chaotic behavior in the case of, say, a triangular billiard with angles which are irrational fractions of π | a chaotic behavior also not due to a local separation of trajectories in phase space, but rather to the eventual emergence of a different pattern of reflections (indeed of any two such billiard trajectories, however close their initial data, one shall eventually miss a reflection near a corner which the other one does take, and from that moment their time evolutions become quite different).

A different possibility, which we consider unlikely but we cannot a priori exclude at this stage of our analysis, is that nonperiodic solutions $z(t)$ of (2.1a) exist which are associated with a Riemann surface of the corresponding solutions $z(t)$ of (2.5) that, even though it possesses an infinite number of relevant branch points inside the circular contour C , it features all of them | or at least most of them, except possibly for a finite number of them | located in a region well inside C , namely separated from it by an annulus of finite thickness. Clearly in such a case two nonperiodic solutions $z(t)$ of (2.1a) which emerge from sufficiently close initial data separate slowly and gradually throughout their time evolution, hence they do not display a sensitive dependence on their initial data | hence, in such a case there would be solutions which are nonperiodic (nor, of course, multiply periodic) but which nevertheless do not display a chaotic behavior | or, to be more precise, there would be sets of initial data, having nonvanishing measure in the phase space of initial data, which yield such nonperiodic (yet nonchaotic) solutions.

As indicated by its title, this paper is mainly focussed on the periodic solutions. In the following Section 5 the analysis of their phenomenology given in this section is complemented by the display of numerical simulations. We shall also exhibit solutions which appear nonperiodic and perhaps chaotic, although such characteristics can of course never be demonstrated with complete cogency via numerical examples.

5 Periodicity of the solutions of the system of ODEs (2.1a): numerical simulations

In this section we display several numerical solutions of the Newtonian equations of motion (2.1a) with

$$\lambda = 2 \quad (5.1a)$$

hence (see (2.2))

$$T = 1: \quad (5.1b)$$

These results confirm graphically the findings discussed in the preceding Section 4. The strategy of our presentation is to exhibit a sequence of numerically-computed solutions of (2.1a) with (5.1a) corresponding to different choices of initial data, for various models

characterized by an assignment of the number N of particles and of the values of the coupling constants g_{nm} (that are always assumed to satisfy the symmetry property (1.2b), $g_{nm} = g_{mn}$). For obvious reasons of simplicity, see below, we restrict consideration to $N = 3$ and $N = 4$. For each model we consider sequences of motions characterized by sets of initial data linked to each other by the formulas

$$x_n(0) = x_n^{(0)}; \quad y_n(0) = y_n^{(0)}; \quad (5.2a)$$

$$\tilde{x}_n(0) = x_n^{(0)} + 2(\tilde{y}_n^{(0)} - y_n^{(0)}); \quad \tilde{y}_n(0) = y_n^{(0)} + 2(\tilde{x}_n^{(0)} - x_n^{(0)}); \quad (5.2b)$$

of course with $z_n = x_n + iy_n$. Here $\tilde{}$ is a positive rescaling parameter the different values of which identify different sets of initial data (while the data $x_n^{(0)}, y_n^{(0)}, \tilde{x}_n^{(0)}, \tilde{y}_n^{(0)}$ are kept fixed). The motivation for such a choice is that, as it can be easily verified by rescaling appropriately the dependent and independent variables (see (2.3) and (2.6) with (5.1a)), these sets of initial data (5.2) identify different solutions $\underline{z}(t)$ of the system of ODEs (2.1a) with (5.1a) that correspond to different solutions $\underline{z}(\tau)$ of the system of ODEs (2.5) related to each other by the following change of initial data,

$$\underline{z}(\tau) = \tilde{\underline{z}}(\tau); \quad \tilde{\underline{z}}(0) = \underline{z}(0); \quad (5.2c)$$

This, as can be easily verified, entails these solutions $\underline{z}(\tau)$ are related to each other merely via a rescaling of dependent and independent variables by a constant factor. Hence all these solutions are associated to the same Riemann surface except for a shrinking of the complex τ -plane by a common factor $|\tilde{}|$ which, as can be readily verified, is just $\tilde{}^2$. Therefore, in the context of the discussion of the preceding Section 4, to analyze the motions yielded by the initial data (5.2) one can just imagine to multiply the diameter of the circle C by the factor $\tilde{}^2$ without modifying the Riemann surface Σ so that larger values of $\tilde{}$ entail that more branch points fall within C .

So for small enough values of $\tilde{}$ — namely for initial conditions characterized by large particle coordinates hence by large interparticle separation and by large initial velocities almost "orthogonal" to the initial positions (see (5.2a,b)) — the circle C shrinks to a small enough radius so that it contains no branch points, hence the corresponding motion (solution of (2.1a) with (5.2a,b)) is completely periodic with period $T = 1$, see (4.1a) and (5.1b), and moreover it features the symmetry property (4.1b). As $\tilde{}$ gets increased one goes through the scenarios described in Section 4 — since, as we concluded above, such an increase can be interpreted as amounting merely to an increase of the radius of the circle C , causing thereby more and more branch points to be enclosed by it. For very large $\tilde{}$ this process can cause all branch points to be enclosed inside C , a situation which is of course equivalent, as regards the periodicity of the solutions of (1.1) as functions of the real time variable t , to all of them being outside C — hence the expectation, that for very large $\tilde{}$ the motion be again completely periodic with period $T = 1$ and also symmetrical, see (4.1a), (4.1b) (but this need not necessarily happen, since the possibility that the solution $\underline{z}(\tau)$ possesses branch points at infinity cannot be excluded). This expectation is indeed confirmed by some of the examples reported below, while in other cases for very large $\tilde{}$ the numerical simulations become too difficult to be performed reliably, and the corresponding trajectories become unsuitable for transparent display — note that for very large $\tilde{}$ the particles are initially all very close to the origin (hence to each other) and with large initial velocities, see (5.2a,b).

But in this paper we do not elaborate on the numerical aspects, except to reassure the skeptic reader that we made sure in each case of the reliability of the results presented below; we refer for more details to [6]. Let us however note that, while one might think that a useful check of the accuracy of the computation is provided by a verification that the numerically evaluated coordinates $z_n(t)$ indeed imply that the collective coordinates $z(t)$ respectively $z^{(2)}(t)$, see (2.7a) respectively (2.8a), evolve periodically with periods $T = 1$ respectively $T = 2 = 1/2$ according to (2.7c) respectively (2.8c), these tests are in fact not at all cogent: indeed, even poorly evaluated coordinates $z_n(t)$ tend to yield collective coordinates $z(t)$ and $z^{(2)}(t)$ that evolve properly. This happens because the equations of motion that determine the evolution of the collective coordinates $z(t)$ and $z^{(2)}(t)$ are in fact so simple (see (2.7) and (2.8)), that numerical errors made in the integration of (2.1a) tend to cancel out when $z(t)$ and $z^{(2)}(t)$ are evaluated.

Let us also note that, in all the examples considered below, we assigned for simplicity real integer values to the coupling constants; but we did check in every case that the qualitative character of the motions does not change if these coupling constants are replaced by (neighboring) values which are neither entire nor real.

The first example we consider is characterized by the following parameters:

$$N = 3; \quad g_{12} = g_{21} = 1; \quad g_{23} = g_{32} = 10; \quad g_{31} = g_{13} = 2; \quad (5.3a)$$

and by the following values of the parameters $x_n^{(0)}, y_n^{(0)}, \bar{x}_n^{(0)}, \bar{y}_n^{(0)}$ characterizing the initial data via (5.2):

$$\begin{aligned} x_1^{(0)} &= 1; & y_1^{(0)} &= 0; & \bar{x}_1^{(0)} &= 0; & \bar{y}_1^{(0)} &= 1; \\ x_1^{(0)} &= 0; & y_1^{(0)} &= 1; & \bar{x}_1^{(0)} &= 2; & \bar{y}_1^{(0)} &= 0; \\ x_1^{(0)} &= 0.5; & y_1^{(0)} &= 0.5; & \bar{x}_1^{(0)} &= 1; & \bar{y}_1^{(0)} &= 0; \end{aligned} \quad (5.3b)$$

The following Table 5.1 provides an overview of the main features (periodicity, symmetry) of the motions that emerge from initial data determined by (5.2) with (5.2a), as well as an indication of the figures (if any) where the corresponding trajectories are displayed. Here and always below the trajectories of particle 1, 2 respectively 3 are shown in red, green, respectively blue (and below, those of particle 4 in yellow). Whenever we felt such an additional indication might be usefully displayed we indicated with a black diamond the initial position of each particle (at $t = 0$), with a black dot the position at a subsequent time $t = t_1$ (generally chosen to coincide with some fraction of the period, $t_1 = T/p$, with p a conveniently chosen positive integer), and with smaller black dots the position at every subsequent integer multiple of t_1 (namely at $t = t_k = kt_1$, $k = 2, 3, \dots$); in this manner the direction of the motion along the trajectories can be inferred (from the relative positions along the trajectories of the diamond and the larger dot), as well as some indication of the positions of the particles over time, as they move (by counting the dots along the trajectory). Of course a much more satisfactory visualization of the motions is provided by simulations in which the particle motions are displayed as they unfold over time (as in a movie); it is planned to make available soon, via the web, the numerical code suitable to perform such simulations on personal computers [6]. Let us emphasize that such simulations are particularly stunning to watch in the case of high-period trajectories,

which are very complicated (see below), so that the fact that the particles return eventually exactly on their tracks appears quite miraculous and is indeed a remarkable proof of the reliability of the numerical computation.

Table 5.1

	0.5	0.712	0.81	0.85	0.9	0.97	0.974	0.975	0.98	0.99
Period	1	1	1	1	1	HSL	15	15	13	11
Symmetry	Yes	Yes	No	No	No		No	No	No	No
Fig. 5.1	a	b	c		d		e			f

	1	1.01	1.02	1.03	1.04	1.05	1.1	1.2	2	5
Period	9	9	7	5	5	3	1	1	1	1
Symmetry	No	No	No	No	No	No	No	No	No	Yes
Fig. 5.1	g		h	i		j		k		m

Now some comments on these results (see Table 5.1 and the set of Figs. 5.1). For $\mu = 0.712$ there clearly are no singularities inside C , hence the motion is periodic with the basic period $T = 1$, and moreover antiperiodic with period $T = 1/2$, so that all trajectories are symmetrical (see for instance Figs. 5.1a,b). A transition occurs at some value of μ larger than 0.712 but smaller than 0.81, and it causes a branch point to enter inside C , opening the way to a second sheet (of the Riemann surface associated with the solution \underline{z} of (2.5) with (5.3)) and thereby causing the trajectories of the solution $\underline{z}(t)$ of (2.1) to lose their symmetry, while still preserving period $T = 1$. This transition is due to a collision among particles 1 (red) and 3 (blue), occurring at a time of the order of, or maybe a bit less than, $(3=10)T = 3=10$ (see Figs. 5.1b and 5.1c, where clearly $t_1 = T=10 = 1=10$). Another, more dramatic, transition occurs for a value of μ between 0.9 and 0.97, and it causes a major increase in the complication of the motion, perhaps a transition to chaos. This transition is of course due to the entrance inside C of a branch point that opens the way — as the complex variable z travels around and around on the circle C — to a very large number of sheets of the Riemann surface associated with the solution \underline{z} of (2.5) with (5.3), possibly to an infinity of them, resulting in motions that look chaotic: this we indicate in Table 5.1 with the acronym HSL, which stands for "Hic Sunt Leones" — see the column with $\mu = 0.97$. This transition is due again to a collision between particles 1 (red) and 3 (blue), at a time of the order, or maybe a little less, than $(8=10)T = 8=10$ (see Fig. 5.1d, where clearly again $t_1 = T=10 = 1=10$). Further increases of μ cause instead a decrease of the complication of the trajectories, characterized first of all by a return to periodic (if still very complicated, due to the large periods) motions, and subsequently by a progressive decrease of the period (see the relevant graphs, from Fig. 5.1e to Fig. 5.1m); this is of course interpreted as due to the fact that the access to additional sheets of the Riemann surface associated with the solution \underline{z} of (2.5) with (5.3) gets shut off because also the second branch point corresponding to the cut that opened the way to those sheets gets enclosed inside the circle C . Thus the trajectories shown in Fig. 5.1e (corresponding to $\mu = 0.974$; see Table 5.1) are interpreted, on the basis of the discussion of the preceding Section 4, as corresponding to access to 30 sheets altogether of the Riemann surface associated with the solution \underline{z} of (2.5) with (5.3); likewise those shown in Fig. 5.1f (corresponding to $\mu = 0.99$; see Table 5.1) are interpreted as corresponding to access to 22 sheets of the Riemann surface associated with the solution \underline{z} of (2.5) with (5.3); those shown in Fig. 5.1k (corresponding to $\mu = 1.2$; see Table 5.1) are interpreted as corresponding to

access to 2 sheets, and finally those shown in Fig. 5.1m (corresponding to $\ell = 5$; see Table 5.1) are interpreted as corresponding to access to just 1 sheet, namely just the main one.

The second example we consider is characterized by the following parameters:

$$N = 3; \quad g_{12} = g_{21} = 10; \quad g_{23} = g_{32} = 3; \quad g_{31} = g_{13} = 10; \quad (5.4a)$$

and by the following values of the parameters $x_n^{(0)}, y_n^{(0)}, \bar{x}_n^{(0)}, \bar{y}_n^{(0)}$ characterizing the initial data via (5.2):

$$\begin{aligned} x_1^{(0)} &= 1; & y_1^{(0)} &= 0; & \bar{x}_1^{(0)} &= 0; & \bar{y}_1^{(0)} &= 2; \\ x_1^{(0)} &= 0; & y_1^{(0)} &= 1; & \bar{x}_1^{(0)} &= 4; & \bar{y}_1^{(0)} &= 0; \\ x_1^{(0)} &= 0.5; & y_1^{(0)} &= 0.5; & \bar{x}_1^{(0)} &= 0.5; & \bar{y}_1^{(0)} &= 1; \end{aligned} \quad (5.4b)$$

Table 5.2

	0.5	1	1.2	1.5	2	2.2	2.5	3	3.5	4
Period	1	1	HSL	HSL	14	14	17	17	17	17
Symmetry	Yes	No			No	Yes	Yes	Yes	Yes	Yes
Fig. 5.2	a	b			c	d			e	

	4.05	4.15	4.2	4.5	5	10	18	20	30	50
Period	17	10	9	7	7	7	7	7	7	7
Symmetry	Yes	No	No	No	No	Yes	Yes	Yes	Yes	Yes
Fig. 5.2		f	g		h		i			

Since the qualitative picture is analogous to that displayed above, we limit our presentation to the display of Table 5.2 and of the corresponding set of graphs (see Figs. 5.2), letting to the alert reader the fun to repeat the discussion as given above. We merely emphasize that, in contrast to the previous case, we see in this case also trajectories with an even period, as well as some high-period trajectories that are symmetrical (the alert reader will have no difficulty in identifying the number of sheets of the Riemann surface associated with the solution $\underline{\quad}$ () of (2.5) with (5.4), for each of the cases reported in Table 5.2). One is also led to suspect, from the data reported in the last columns of Table 5.2, that the Riemann surface associated with the solution $\underline{\quad}$ () of (2.5) with (5.4) possesses (at least) 7 branch points at or near infinity (of course on different sheets, so that they do not cancel each other).

The third example we consider is a 4-particle one, characterized by the following parameters:

$$\begin{aligned} N &= 4; & g_{12} &= g_{21} = 3; & g_{13} &= g_{31} = 9; & g_{14} &= g_{41} = 12; \\ g_{23} &= g_{32} = 9; & g_{24} &= g_{42} = 12; & g_{34} &= g_{43} = 3; \end{aligned} \quad (5.5a)$$

and by the following values of the parameters $x_n^{(0)}, y_n^{(0)}, \bar{x}_n^{(0)}, \bar{y}_n^{(0)}$ characterizing the initial data via (5.2):

$$\begin{aligned} x_1^{(0)} &= 2.4; & y_1^{(0)} &= 0; & \bar{x}_1^{(0)} &= 0; & \bar{y}_1^{(0)} &= 1; \\ x_1^{(0)} &= 2.4; & y_1^{(0)} &= 0; & \bar{x}_1^{(0)} &= 2; & \bar{y}_1^{(0)} &= 2; \\ x_1^{(0)} &= 0; & y_1^{(0)} &= 0.5; & \bar{x}_1^{(0)} &= 0.5; & \bar{y}_1^{(0)} &= 2; \\ x_1^{(0)} &= 0.5; & y_1^{(0)} &= 0.5; & \bar{x}_1^{(0)} &= 0.5; & \bar{y}_1^{(0)} &= 1; \end{aligned} \quad (5.5b)$$

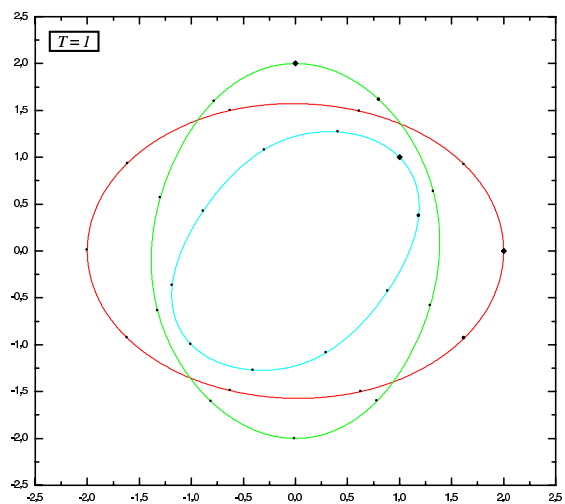


Fig. 5.1a

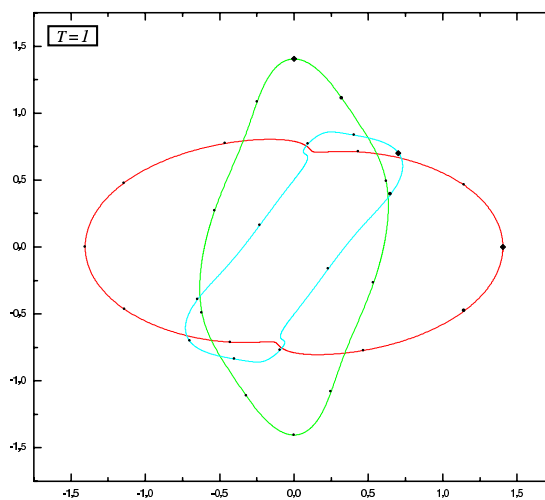


Fig. 5.1b

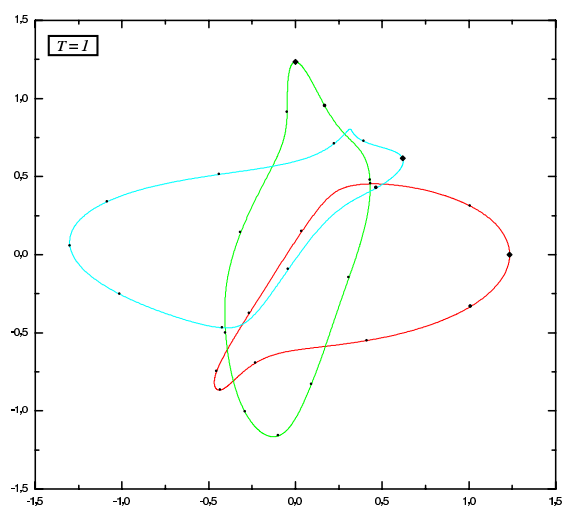


Fig. 5.1c

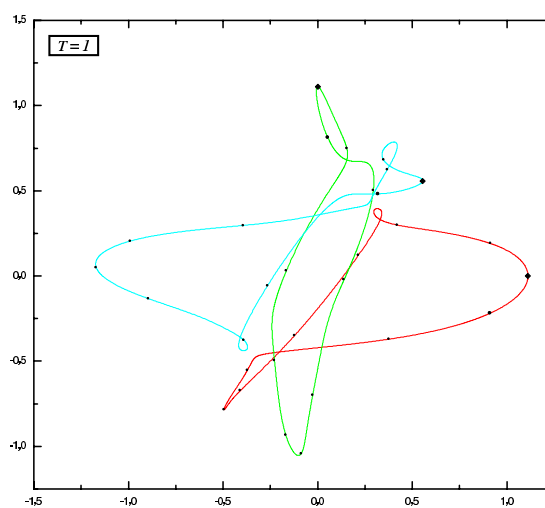


Fig. 5.1d

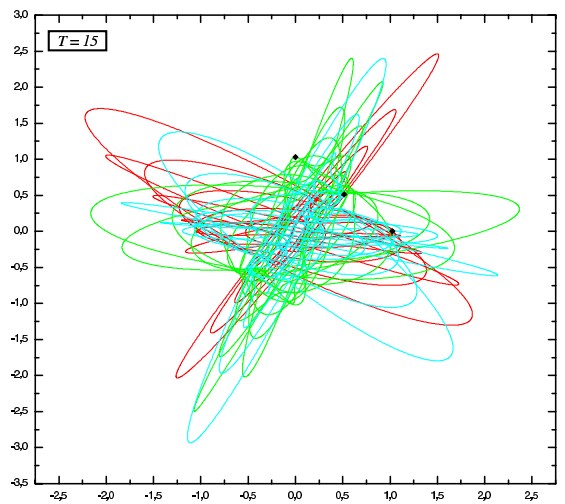


Fig. 5.1e

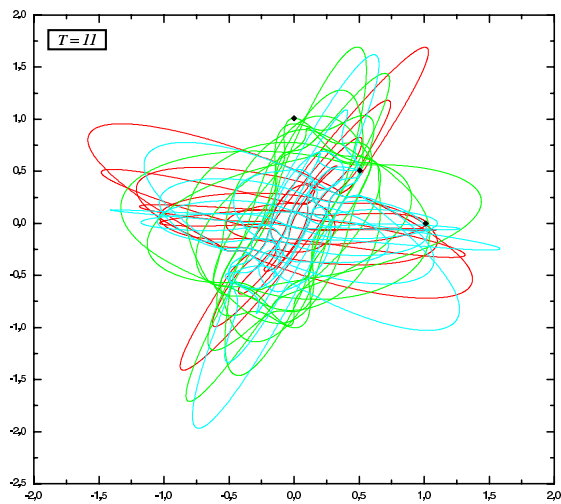


Fig. 5.1f

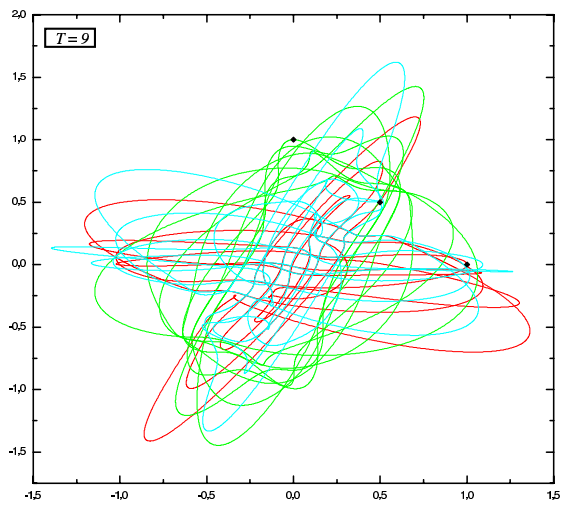


Fig. 5.1g

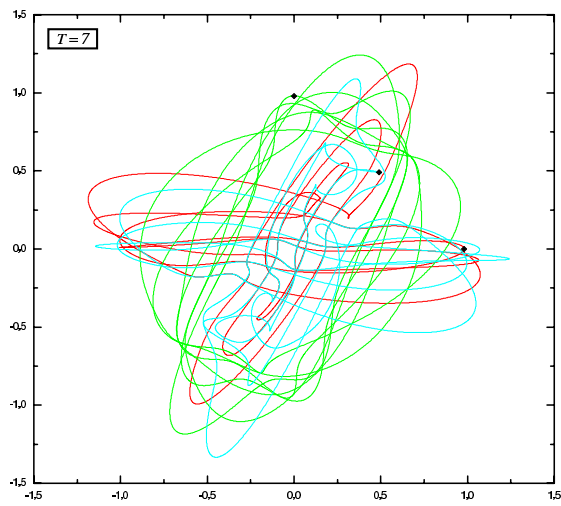


Fig. 5.1h

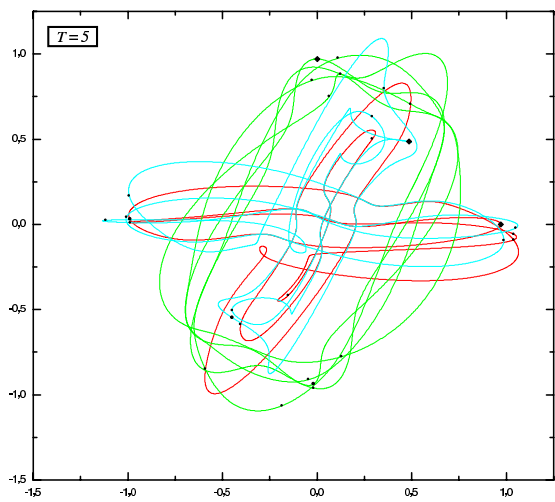


Fig. 5.1i

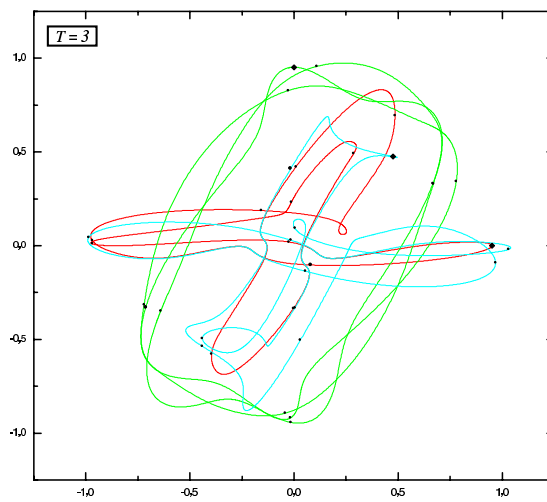


Fig. 5.1j

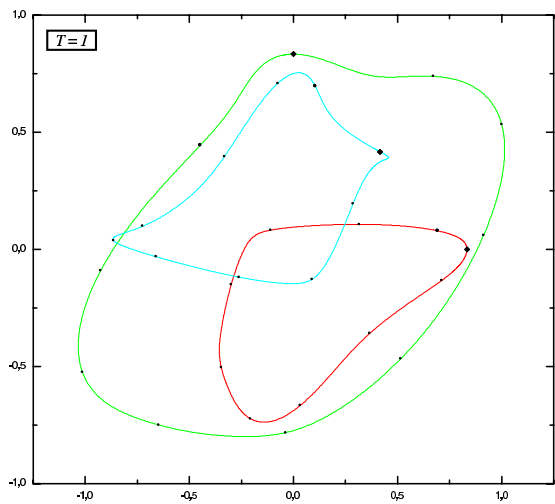


Fig. 5.1k

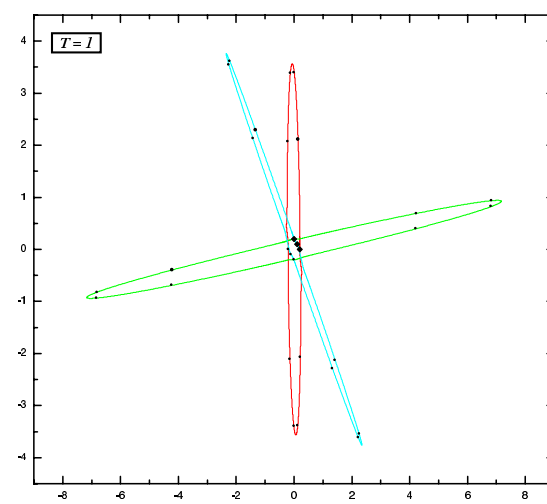


Fig. 5.1m

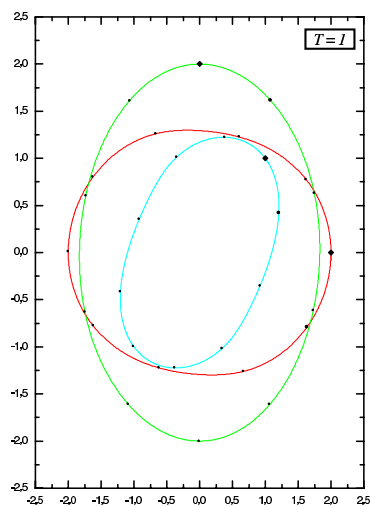


Fig. 5.2a

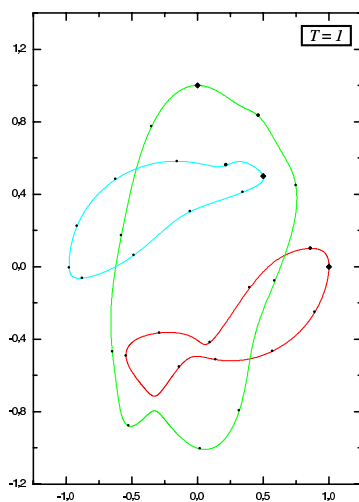


Fig. 5.2b

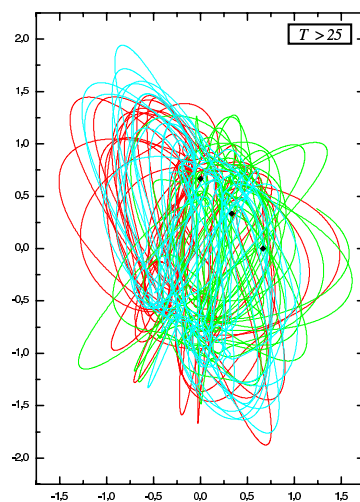


Fig. 5.2c

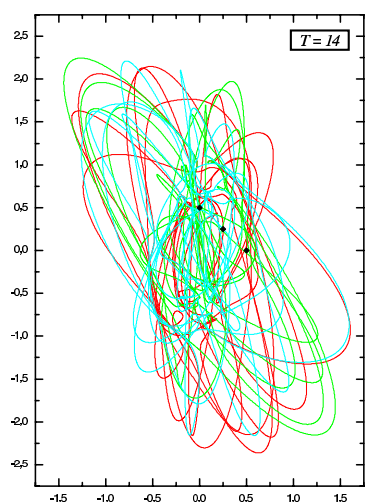


Fig. 5.2d

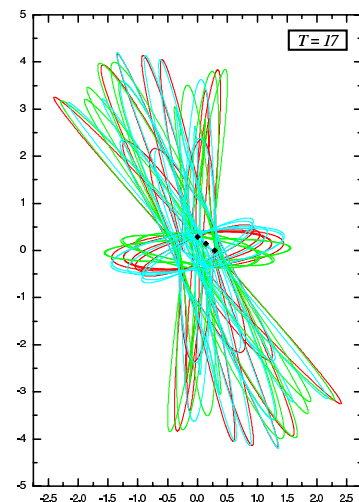


Fig. 5.2e

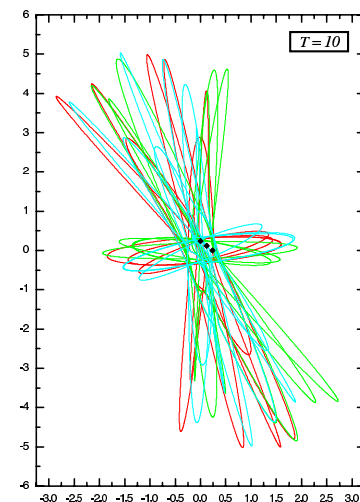


Fig. 5.2f

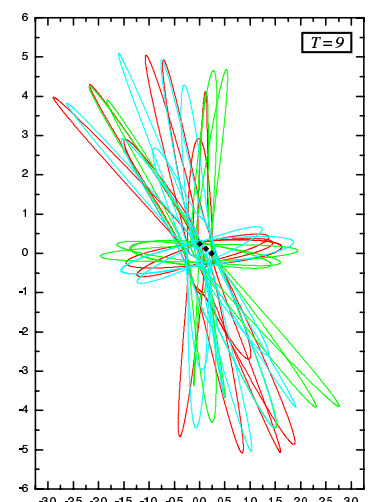


Fig. 5.2g

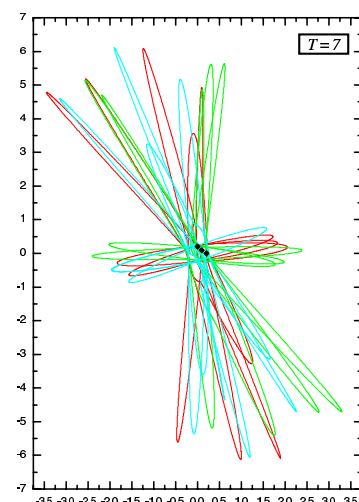


Fig. 5.2h

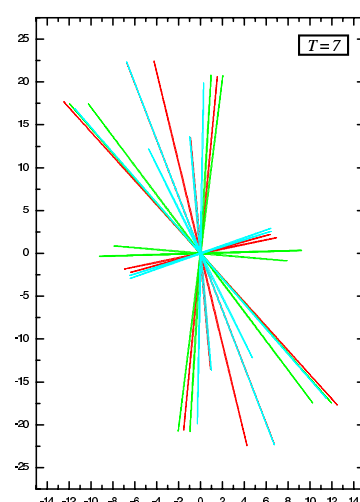


Fig. 5.2i

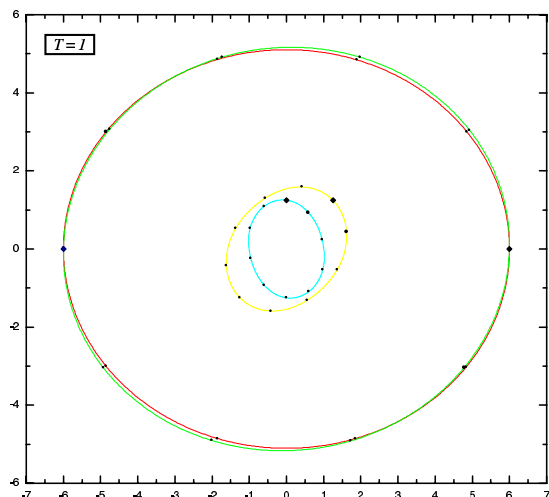


Fig. 5.3a

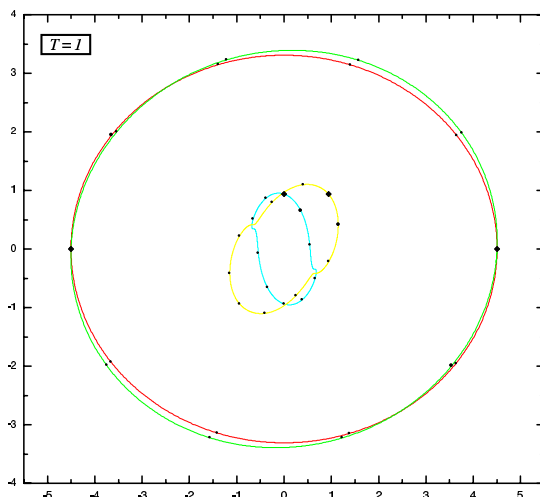


Fig. 5.3b

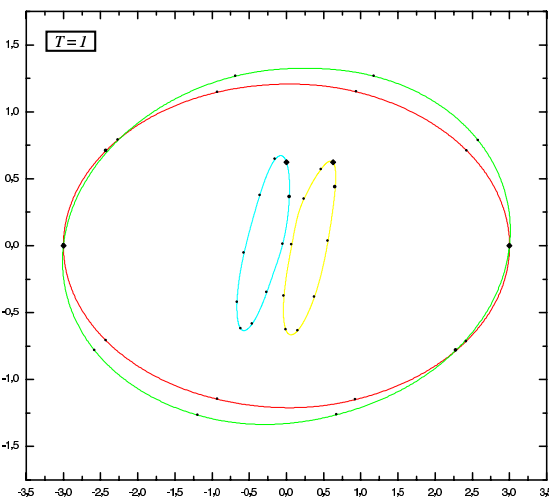


Fig. 5.3c

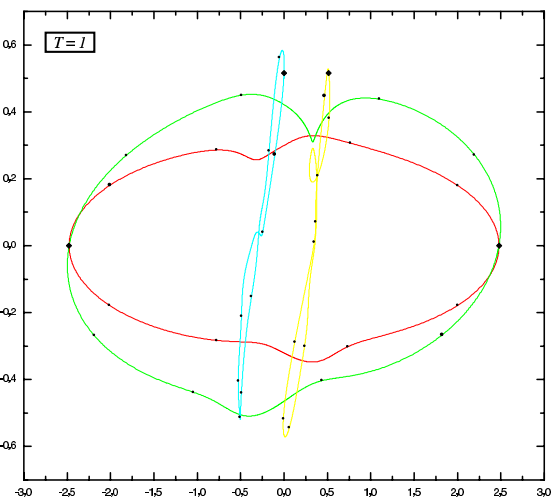


Fig. 5.3d

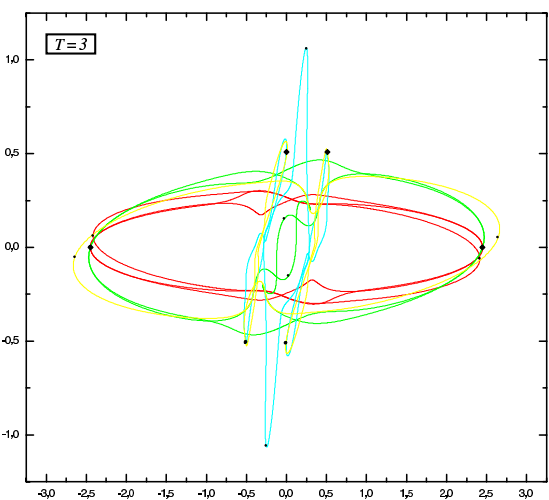


Fig. 5.3e

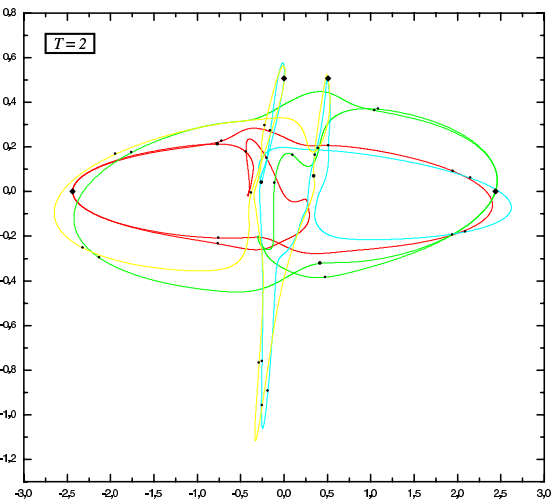


Fig. 5.3f

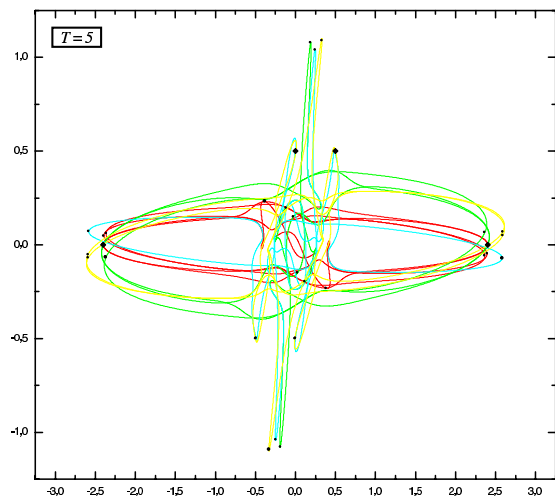


Fig. 5.3g

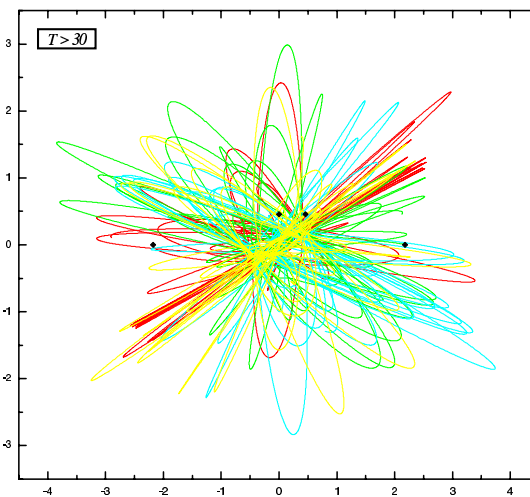


Fig. 5.3h

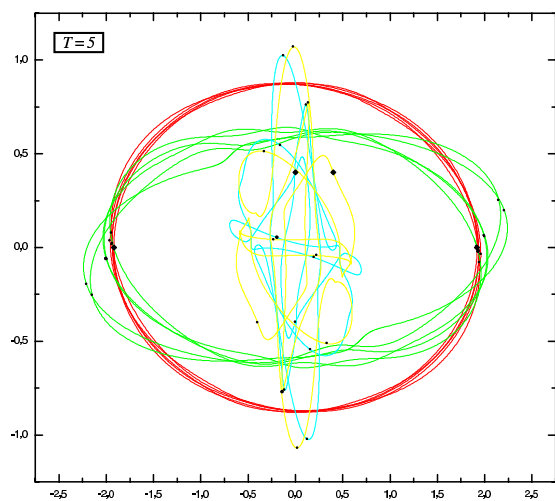


Fig. 5.3i

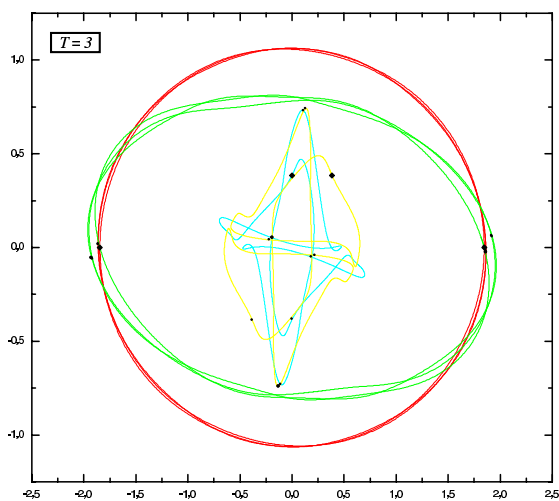


Fig. 5.3j

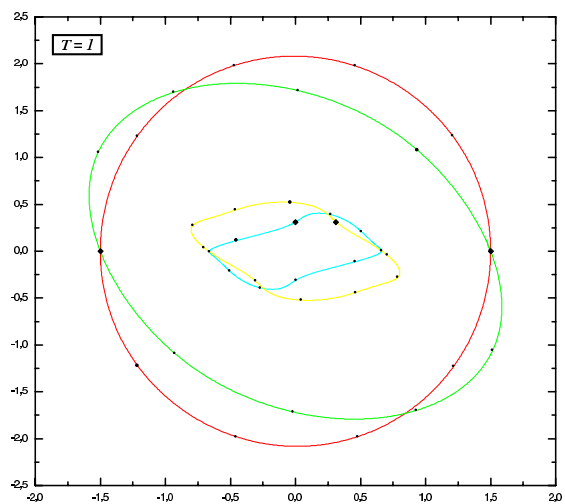


Fig. 5.3k

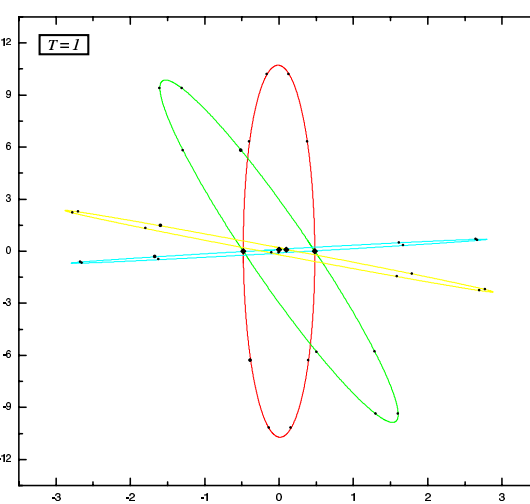


Fig. 5.3m

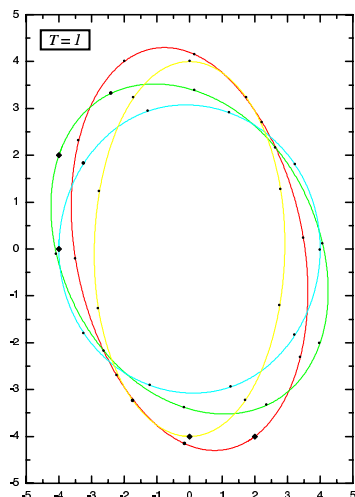


Fig. 5.4a

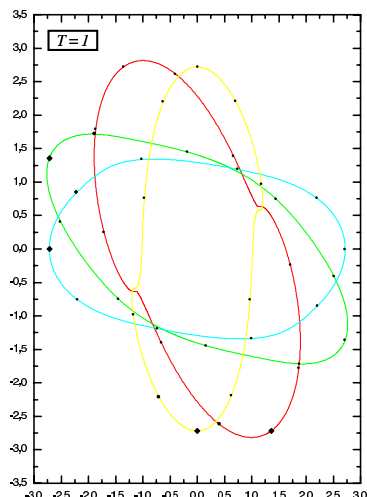


Fig. 5.4b

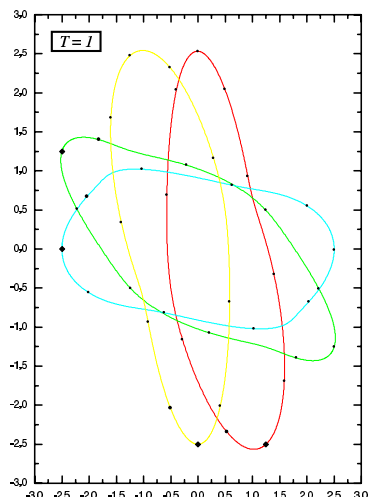


Fig. 5.4c

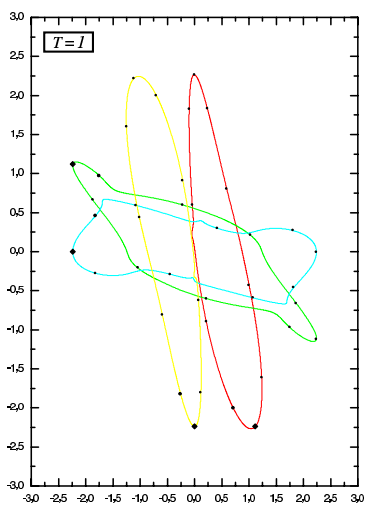


Fig. 5.4d

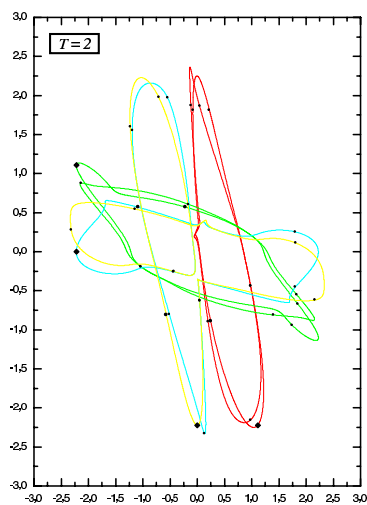


Fig. 5.4e

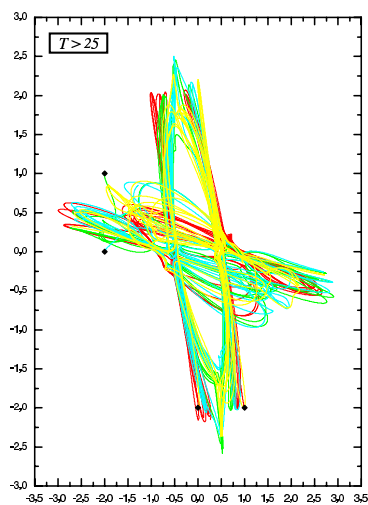


Fig. 5.4f

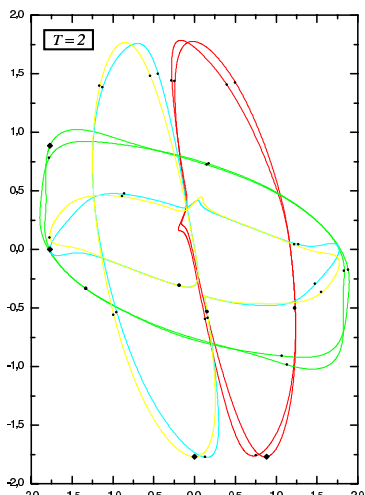


Fig. 5.4g

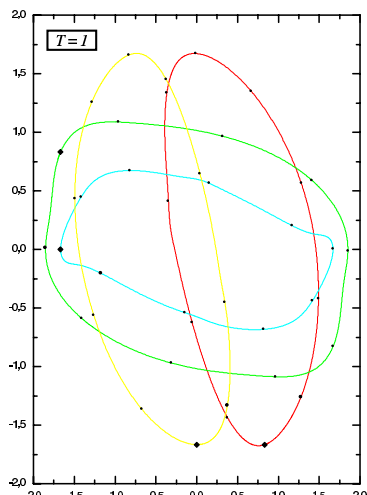


Fig. 5.4h

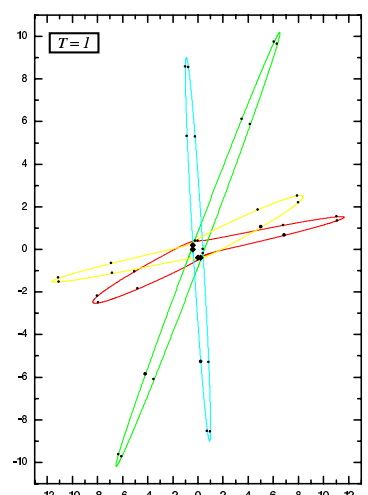


Fig. 5.4i

A representative selection of our findings is reported in Table 5.3, and some of the corresponding trajectories are displayed in the Figures as indicated there.

Table 5.3

	0.4	0.533	0.8	0.9	0.9687	0.98	0.985	0.99	1
Period	1	1	1	1	1	3	2	5	5
Symmetry	Yes	Yes	No	No	No	Yes	No	Yes	Yes
Fig. 5.3	a	b	c		d	e	f		g

	1.01	1.1	1.225	1.25	1.3	1.5	1.6	2	5	10
Period	HSL	HSL	HSL	5	3	1	1	1	1	1
Symmetry				Yes	Yes	Yes	Yes	Yes	Yes	Yes
Fig. 5.3		h		i	j		k		m	

For $\gamma = 0.533$ we have no singularities inside \tilde{C} , hence the motion is periodic with the basic period $T = 1$, and moreover antiperiodic with period $T = 1/2$, so that all trajectories are symmetrical (see Figs. 5.3a,b). A transition occurs at some value of γ between 0.533 and 0.8, due to a collision among particles 3 (blue) and 4 (yellow), occurring at a time of the order of, or maybe a bit less than, $(3=10)T = 3=10$ (see Figs. 5.3b and 5.3c, where clearly $t_1 = T=10 = 1=10$). Another transition occurs for a value of γ greater than 0.9687 but less than 0.98, and it causes a branch point to enter inside \tilde{C} at some value of γ between 0.8 and 0.9687, opening thereby the way to a third sheet of the Riemann surface associated with the solution $\underline{\psi}(\cdot)$ of (2.5) with (5.5). This second transition is due to a collision, in this case among particles 2 (green) and 4 (yellow), occurring at a time of the order, or maybe a little less, than $(8=10)T = 8=10$ (see Fig. 5.1d, where clearly again $t_1 = T=10 = 1=10$). Then two more transitions occur (see Fig. 5.3e,f,g) — one for γ between 0.98 and 0.985, the other for γ between 0.985 and 0.99 — each opening the way to one more sheet of the Riemann surface associated with the solution $\underline{\psi}(\cdot)$ of (2.5) with (5.5) (recall the discussion of Section 4: overall access to P sheets including the main one, $P = 1 + B$ in the notation of Section 4, yields a completely periodic symmetrical motion with period P if P is odd — with every sheet being visited twice in each period; it yields a completely periodic unsymmetrical motion with period $P=2$ if P is even — with every sheet being visited once in each period: hence for the trajectories shown in Figs. 5.3a,b $P = 1$, for those shown in Figs. 5.3c,d $P = 2$, for those shown in Fig. 5.3e $P = 3$, for those shown in Fig. 5.3f $P = 4$, for those shown in Fig. 5.3g $P = 5$). A more dramatic transition occurs for a value of γ between 1 and 1.01, and it causes a major increase in the complication of the motion, perhaps a transition to chaos (see Fig. 5.3h). Like in the first example, and of course due to the same mechanism as discussed above, further increases of γ ($\gamma > 1.225$) cause instead a decrease of the complication of the trajectories, characterized first of all by a return to periodic motions, and subsequently by a progressive decrease of the period (see Figs. 5.3i,m).

The fourth and last example we report is characterized by the following parameters:

$$\begin{aligned} N &= 4; & g_{12} &= g_{21} = 5; & g_{13} &= g_{31} = 10; & g_{14} &= g_{41} = 20; \\ g_{23} &= g_{32} = 20; & g_{24} &= g_{42} = 10; & g_{34} &= g_{43} = 5; \end{aligned} \quad (5.6a)$$

and by the following values of the parameters $x_n^{(0)}, y_n^{(0)}, \bar{x}_n^{(0)}, \bar{y}_n^{(0)}$ characterizing the initial

data via (5.2):

$$\begin{aligned}
 x_1^{(0)} &= 1; & y_1^{(0)} &= 2; & x_1^{(0)} &= 0; & y_1^{(0)} &= 1; \\
 x_1^{(0)} &= 2; & y_1^{(0)} &= 1; & x_1^{(0)} &= 1; & y_1^{(0)} &= 1; \\
 x_1^{(0)} &= 2; & y_1^{(0)} &= 0; & x_1^{(0)} &= 0; & y_1^{(0)} &= 1; \\
 x_1^{(0)} &= 0; & y_1^{(0)} &= 2; & x_1^{(0)} &= 1; & y_1^{(0)} &= 0;
 \end{aligned} \tag{5.6b}$$

A representative selection of our findings is reported in Table 5.4, and some of the corresponding trajectories are displayed in the Figs. 5.4 as indicated there.

Table 5.4

	0.5	0.736	0.8	0.894	0.9	0.904	0.905	0.91	0.95
Period	1	1	1	1	2	2	HSL	HSL	HSL
Symmetry	Yes	Yes	No	No	No	No			
Fig. 5.4	a	b	c	d	e				

	1	1.1	1.125	1.13	1.15	1.2	1.5	2	5	10
Period	HSL	HSL	2	2	1	1	1	1	1	1
Symmetry			No	No	No	No	No	No	No	No
Fig. 5.4	f			g		h			i	

Since the qualitative picture is analogous to those displayed above, we limit our presentation to the display of Table 5.4 and of the corresponding set of Figs. 5.4, letting to the alert reader the fun to repeat the discussion as given above.

6 Outlook

The results proven in this paper provide an additional explicit instance of a phenomenon whose rather general scope has been already advertized via a number of other examples, treated elsewhere in more or less complete detail [14].

An analogous treatment to that given in this paper will be published soon [5] in the context of the "generalized gold sh model" [8, 2], which is somewhat richer inasmuch as it features branch points the nature of which depends on the values of the coupling constants (in contrast to the case treated herein, where all relevant branch points are of square-root type), and has moreover the advantage that its treatment in the C_N context is directly interpretable as a genuine (i.e., rotation-invariant) real many-body problem in the plane (as discussed at the end of the introductory Section 1, this is not the case for the model considered herein — although there does exist a modified version of it in which this "defect" is eliminated [9]). On the other hand the class of many-body problems with inverse-cube interparticle potentials, as considered herein, have been (especially, of course, in the integrable version with equal coupling constants) much studied over the last quarter century, while the "gold sh" model has not yet quite acquired a comparable "classical" status.

Of course a more detailed, if perhaps less "physical", understanding of the dynamics of the model studied herein might be gained by investigating numerically the solutions $_{()}$ of the equations of motion (2.5) as functions of the complex variable (rather than the

solutions $\underline{z}(t)$ as functions of the real variable t), and in particular by mapping out the detailed shape of the multi-sheeted Riemann surfaces associated with these solutions; and analogous considerations apply to all the models [15] in which the "trick", see Section 2, plays a key role. This remains as a task for the future.

Acknowledgments

While the results reported in this and related papers were under development we discussed them with several colleagues, who often provided precious suggestions. In particular we like to thank for these Robert Conte, Ovidiu Costin, Herman Flaschka, Giovanni Gallavotti, Nalini Joshi, Martin Kruskal, Francois Leyvraz, Orlando Ragnisco and Alexander Turbiner.

Appendix A : the ansatz (3.2)

In this appendix we show that the ansatz (3.2) is consistent with the ODEs (2.5), and that the requirement that (3.2) satisfy (2.5) allows to determine uniquely the coefficient and in principle as well all the coefficients $g_l^{(n)}$ featured by this ansatz, while the remaining coefficients, namely the 4 constants b, v, a and b_0 in (3.2a), (3.2b), and the $2(N-2)$ constants b_n, v_n in (3.2c), remain arbitrary (except for the obvious requirements $b_n \neq b, b_n \neq b_m$, which are hereafter assumed to hold).

Indeed the insertion of (3.2) in (2.5) with $n=1$ respectively $n=2$ yields

$$\begin{aligned} & \frac{1}{4} (b_0)^{3=2} + \frac{3}{4} a (b_0)^{1=2} + \sum_{l=4}^X \frac{l(l-2)}{4} g_l^{(1)} (b_0)^{(l-4)=2} \\ & = g_{12} (2)^3 (b_0)^{3=2} \left(1 + \frac{a}{b_0} \right) + \sum_{l=4}^X \frac{1}{2} g_l^{(1)} g_l^{(2)} (b_0)^{(l-1)=2} \\ & + \sum_{m=1; m \neq n}^X g_{1m} (b_0 - b_m)^3 \left(1 + (b_0 - b_m)^{-1} (b_0)^{1=2} + (v - v_m) (b_0) \right. \\ & \left. + a (b_0)^{3=2} + \sum_{l=4}^X \frac{l}{1} g_l^{(1)} g_l^{(m)} (b_0)^{l=2} \right) \quad (\text{A } 1a) \end{aligned}$$

respectively

$$\begin{aligned} & \frac{1}{4} (b_0)^{3=2} - \frac{3}{4} a (b_0)^{1=2} + \sum_{l=4}^X \frac{l(l-2)}{4} g_l^{(2)} (b_0)^{(l-4)=2} \\ & = g_{12} (2)^3 (b_0)^{3=2} \left(1 + \frac{a}{b_0} \right) + \sum_{l=4}^X \frac{1}{2} g_l^{(1)} g_l^{(2)} (b_0)^{(l-1)=2} \\ & + \sum_{m=1; m \neq n}^X g_{2m} (b_0 - b_m)^3 \left(1 + (b_0 - b_m)^{-1} (b_0)^{1=2} + (v - v_m) (b_0) \right. \\ & \left. + a (b_0)^{3=2} + \sum_{l=4}^X \frac{l}{1} g_l^{(1)} g_l^{(m)} (b_0)^{l=2} \right) \quad (\text{A } 1b) \end{aligned}$$

$$a (b)^{3=2} + \sum_{l=4}^X \frac{(2)}{1} \frac{(m)}{1} (b)^{l=2} : \quad \#) \quad 3 \quad (A.1b)$$

We now equate in each of these two equations the coefficients of the term $(b)^{3=2}$ and we get the (same) relation that determines the coefficient ,

$$= (g_{12}=2)^{1=4} : \quad (A.2)$$

And we also see that, with this assignment of , in both equations, (A.1a), (A.1b), the terms that multiply $(b)^{1=2}$ also match exactly.

It is also easily seen that the remaining terms can be matched recursively (by expanding the right-hand sides of these equations, (A.1a), (A.1b) | as well as those of (A.1c), see below | in powers of $(b)^{1=2}$), and that in this manner the coefficients $\frac{(1)}{1}, \frac{(2)}{1}$ get uniquely determined, for instance

$$\frac{(j)}{4} = \sum_{m=3}^X [(13g_{jm} - 3g_{j+1,m})=20] (b - b_m)^3 ; \quad j = 1; 2 \text{ mod } (2) : \quad (A.3a)$$

To complete the analysis one must also check the remaining equations (2.5), with $n > 2$. Insertion of the ansatz (3.2) in these yields

$$\begin{aligned} & \sum_{l=4}^X \frac{1(l-2)}{4} \frac{(n)}{1} (b)^{(l-4)=2} \\ & = g_{n1} (b_n - b)^3 + 1 + (b_n - b)^1 (b)^{1=2} + (v_n - v) (b) \\ & + a (b)^{3=2} + \sum_{l=4}^X \frac{(n)}{1} \frac{(1)}{1} (b)^{l=2} \\ & + g_{n2} (b_n - b)^3 + 1 + (b_n - b)^1 (b)^{1=2} + (v_n - v) (b) \\ & + a (b)^{3=2} + \sum_{l=4}^X \frac{(n)}{1} \frac{(2)}{1} (b)^{l=2} \\ & + \sum_{m=1; m \neq n}^X g_{nm} (b_n - b_m)^3 + 1 + (b_n - b_m)^1 (v_n - v_m) (b) \\ & + \sum_{l=4}^X \frac{(n)}{1} \frac{(m)}{1} (b)^{l=2} ; \quad n = 3; 4; \dots; N : \quad \#) \quad 3 \quad (A.1c) \end{aligned}$$

The consistency of these equations is plain, as well as the possibility they entail to compute in principle | in conjunction with (A.1b), (A.1c) | the coefficients $\frac{(n)}{1}$. For instance one immediately obtains

$$\begin{aligned} \frac{(n)}{4} & = \frac{1}{2} \sum_{m=3; m \neq n}^X (g_{n1} + g_{n2}) (b_n - b)^3 + \sum_{m=3; m \neq n}^X g_{nm} (b_n - b_m)^3 ; \\ n & = 3; 4; \dots; N : \quad (A.3b) \end{aligned}$$

The treatment of the multiple-collision case, see (3.1b), via the corresponding ansatz, (3.3), is closely analogous, but in this case the matching of the coefficients of the terms proportional to $(b)^{3=2}$ respectively to $(b)^{1=2}$ yields

$$g_{nm} = \frac{1}{4} \sum_{m=1; m \neq n}^M g_{nm} (b_n - b_m)^3; \quad n = 1; 2; \dots; M; \quad (\text{A } 4a)$$

$$a_n = \frac{1}{4} \sum_{m=1; m \neq n}^M g_{nm} (b_n - b_m)^4 (a_n - a_m); \quad n = 1; 2; \dots; M; \quad (\text{A } 4b)$$

So in this case the coefficients g_{nm} and a_n get fixed by these algebraic equations (up, for the coefficients a_n , to a common factor). But the basic conclusion about the square-root nature of the branch points is confirmed, as indeed entailed by the ansatz (3.3).

And it can be easily verified that analogous conclusions also obtain in the case of more general multiple collisions in which the coordinates collide in groups, for instance

$$\begin{aligned} b_1(b) = b_2(b); \quad b_3(b) = b_4(b) = b_5(b); \quad b_n(b) \neq b_1(b); \\ b_n(b) \neq b_3(b); \quad b_n(b) \neq b_m(b); \quad n; m = 6; 7; \dots; N; \end{aligned} \quad (\text{A } 5)$$

the appropriate ansatz being in this case of type (3.3a) for the colliding coordinates $b_n(b)$, $n = 1; 2; \dots; 5$ (with the same values of the constants b and v for each subgroup of colliding coordinates, say, in self-evident notation, $b_1 = b_2, b_3 = b_4 = b_5, v_1 = v_2, v_3 = v_4 = v_5$), of type (3.3b) for the non colliding coordinates $b_n(b)$, $n = 6; 7; \dots; N$.

Appendix B : the three-body case

In this appendix we discuss the solution of the evolution equations (2.5) in the three-body case, $N = 3$. As we show below the solution of this three-body problem can be reduced to quadratures. This fact was discovered by C. Jacobi almost two centuries ago (but this finding was only published after his death [10]), was then rediscovered by C. Marchioro (who also did not publish this finding) and was finally neatly presented by D. C. Khundekar and S. V. Lawande [11], who actually treated (2.1a) rather than (2.5) (they were not aware at the time of the "trick" (2.4) that relates (2.5) to (2.1a), and they mainly focussed on the integrable case with equal coupling constants and on its connection with the corresponding quantal problem — for a bit more on the history of this problem see Section 2.N of Ref. [2]).

So we now focus on the evolution equations

$$g_{nm} = \frac{1}{4} \sum_{m=1; m \neq n}^3 g_{nm} (b_n - b_m)^3; \quad n = 1; 2; 3; \quad g_{nm} = g_{mn}; \quad b_n = b_n(b); \quad (\text{B } 1)$$

which clearly obtain from the Hamiltonian

$$H = \frac{1}{2} (p_1^2 + p_2^2 + p_3^2) + \frac{1}{2} (g_{12} (b_1 - b_2)^2 + g_{23} (b_2 - b_3)^2 + g_{31} (b_3 - b_1)^2) \quad (\text{B } 2a)$$

hence entail that the quantity

$$H = \frac{1}{2} (p_1^2 + p_2^2 + p_3^2) + \frac{1}{2} (g_{12} (b_1 - b_2)^2 + g_{23} (b_2 - b_3)^2 + g_{31} (b_3 - b_1)^2) \quad (\text{B } 2b)$$

is a constant of the motion. It is also plain that the initial position, $\mathbf{r}(0)$, and the (initial) velocity, \mathbf{V} , of the center of mass

$$= (\mathbf{r}_1 + \mathbf{r}_2 + \mathbf{r}_3)/3; \quad (\text{B } 3)$$

are two additional constants of motion, since the evolution equations (B.1) clearly entail that the center of mass moves uniformly:

$$\mathbf{r}(t) = \mathbf{r}(0) + \mathbf{V}t; \quad (\text{B } 4)$$

And we moreover now know (see the last part of Section 2) that the quantity

$$L^{(2)} = \frac{1}{2} \dot{\mathbf{r}}_1^2 + \frac{1}{2} \dot{\mathbf{r}}_2^2 + \frac{1}{2} \dot{\mathbf{r}}_3^2 = 3 \quad (\text{B } 5a)$$

evolves according to the simple equation (see (2.8b))

$$(L^{(2)})^0 = (4/3)H; \quad (\text{B } 5b)$$

with H defined by (B.2b).

It is now convenient [11] to introduce the "Jacobi coordinates"

$$\mathbf{r} = 2^{-1/2} (\mathbf{r}_1 - \mathbf{r}_2); \quad \mathbf{R} = 6^{-1/2} (\mathbf{r}_1 + \mathbf{r}_2 - 2\mathbf{r}_3); \quad (\text{B } 6a)$$

and moreover to introduce the corresponding "circular coordinates" by setting

$$\mathbf{r} = \sin(\theta) \hat{\mathbf{e}}; \quad \mathbf{R} = \cos(\phi) \hat{\mathbf{e}}; \quad (\text{B } 6b)$$

Note that these definitions entail

$$r_1^2 = \frac{1}{2} + 2^{-1/2} \mathbf{r} \cdot \mathbf{R} + 6^{-1/2} \mathbf{R}^2 = (2/3)^{1/2} \cos[\theta + (2/3)\phi]; \quad (\text{B } 7a)$$

$$r_2^2 = \frac{1}{2} - 2^{-1/2} \mathbf{r} \cdot \mathbf{R} + 6^{-1/2} \mathbf{R}^2 = (2/3)^{1/2} \cos[(2/3)\phi - \theta]; \quad (\text{B } 7b)$$

$$r_3^2 = (2/3)^{1/2} = (2/3)^{1/2} \cos \phi; \quad (\text{B } 7c)$$

as well as

$$H = (3/2)V^2 + (1/2)\dot{\theta}^2 + (1/2)\dot{\phi}^2 + (1/4)\dot{\psi}^2 f(\theta, \phi); \quad (\text{B } 8a)$$

$$f(\theta, \phi) = g_{12} \sin^2(\theta) + g_{23} \sin^2[\theta + (2/3)\phi] + g_{31} \sin^2[(2/3)\phi]; \quad (\text{B } 8b)$$

and

$$L^{(2)} = \dot{\mathbf{r}}^2 + (1/3)\dot{\mathbf{R}}^2; \quad (\text{B } 9)$$

From the last formula and (B.4), (B.5b) we get

$$\dot{\mathbf{r}}^2 = 4H - 6V^2; \quad (\text{B } 10a)$$

hence

$$\dot{\mathbf{r}}^2(\theta, \phi) = A^2 + 2B\theta + C = A(\theta + \phi)(\theta - \phi); \quad (\text{B } 10b)$$

$$A = 2H - 3V^2; \quad (\text{B } 10c)$$

$$B = B - D; \quad (\text{B } 10d)$$

$$D^2 = B^2 - C; \quad (\text{B } 10e)$$

Here we have introduced two other constants of integration, B and C , while the constants A and D are defined by (B.10c) and (B.10e).

We now introduce this expression of () in B.8a) and easily obtain the formula

$$\varpi^2 = A^2 D^2 + (1/2)f(\vartheta)^4; \quad (\text{B.11a})$$

that entails the quadrature

$$\int d\vartheta \sqrt{A^2 D^2 - (1/2)f(\vartheta)^4} = \int d\vartheta \sqrt{(\vartheta^2)^2 - 2}: \quad (\text{B.11b})$$

The integral in the right-hand side of this formula, (B.11b), is easily done (see (B.10)), and one arrives thus at the final formula

$$F(\vartheta) = \arccot \left[\frac{(\vartheta + B)/D}{\sqrt{2}} \right]; \quad (\text{B.12a})$$

$$F(\vartheta) = \int d\vartheta \sqrt{1 + (1/2)(AD)^2 f(\vartheta)^4}; \quad (\text{B.12b})$$

where of course $f(\vartheta)$ is defined by (B.8b).

In the integrable "equal-coupling-constants" case,

$$g_{nm} = g; \quad (\text{B.13a})$$

it is easily seen that

$$f(\vartheta) = 9g[\sin(3\vartheta)]^2; \quad (\text{B.13b})$$

hence the integration in the right-hand side of (B.12b) is easily performed to yield

$$F(\vartheta) = (1/3)E - \arcsin[\cos(3\vartheta)g]; \quad (\text{B.13c})$$

where E is an integration constant and

$$= 1 + (9/2)g(AD)^2: \quad (\text{B.13d})$$

Hence in this case one gets for () the completely explicit expression

$$= (1/3) \arccos[\sin fE - 3 \arccot \left[\frac{(\vartheta + B)/D}{\sqrt{2}} \right]]; \quad (\text{B.14})$$

which, together with (B.10b) and (B.4), provides via (B.7) completely explicit expressions of the coordinates $\vartheta_n(\vartheta)$, $n = 1, 2, 3$. From these it is immediately seen that the coordinates $\vartheta_n(\vartheta)$, considered as functions of the complex variable ϑ , feature two kinds of square-root branch points: those occurring at $\vartheta = \vartheta_b$, see (B.10b), (B.10d), which clearly correspond to triple collisions, see (B.10b) and (B.7); and those occurring at $\vartheta = \vartheta_p$,

$$\vartheta_p = B + D \cot \left[\frac{(1/3)E - \arcsin(1/3) + (2/3)k}{g} \right]; \quad k = 0, 1, 2; \quad (\text{B.15})$$

which correspond instead to pair collisions. Indeed it is easily seen that, for ϑ_p ,

$$= (2/3)k + \left[\frac{(\vartheta_p - B)/D}{\sqrt{2}} \right]^{1/2} + O(\vartheta - \vartheta_p); \quad k = 0, 1, 2; \quad (\text{B.16a})$$

$$= i(2/3)^{1/2} \sqrt{1 + (2/9)(AD)^2} g^{1/4} D \sqrt{(\vartheta_p + B)^2 + D^2}; \quad (\text{B.16b})$$

and (B.16a) clearly entails, see (B.7), that a pair collisions occurs at $\theta = \theta_b$.

The analysis of the periodicity of the solutions of (2.1) in this case is plain; of course the fact that the number of branch points is finite entails that in this integrable case all nonsingular solutions are completely periodic, either with period T , see (2.2), or with a period which is a (small) entire multiple of T , confirming the results implied by the general treatment [2] of the integrable equal-coupling-constant N -body problem (2.1).

In the general case with arbitrary coupling constants one can rewrite (B.12b) as follows (by setting $u = 4 \sin^2 \frac{\theta}{2}$):

$$F(\theta) = (1/2) \int_{U(\theta)}^{\infty} du u (1-u)^{1/2} u^2 (u+3+\bar{G}) + G + \hat{G} (3+u)^{3/2} (1-u)^{1/2}; \quad (\text{B.17a})$$

$$\bar{G} = (2g_{12} - g_{23} - g_{31})(AD)^2;$$

$$G = 9(g_{23} + g_{31})(AD)^2; \quad \hat{G} = 3^{1/2}(g_{23} - g_{31})(AD)^2; \quad (\text{B.17b})$$

$$U(\theta) = 4[\sin^2 \frac{\theta}{2} - 3]; \quad (\text{B.17c})$$

In the equal-coupling-constants case, see (B.13a), things simplify because

$$\bar{G} = \hat{G} = 0; \quad (\text{B.18a})$$

see (B.17b), hence the integral in the right-hand side of (B.17) can then be performed in terms of elementary functions, since via the change of variable

$$u^2(u+3) = 4v; \quad (\text{B.18b})$$

somewhat miraculously (albeit not surprisingly) (B.17) yield

$$F(\theta) = (1/3) \int_{W(\theta)}^{\infty} dv f(1-v)(G+v)g^{1/2}; \quad (\text{B.18c})$$

$$W(\theta) = [\sin(3\theta/2)]^2; \quad (\text{B.18d})$$

and of course one gets thereby again (B.13c).

If instead (only) the two coupling constants g_{23} and g_{31} coincide, $g_{23} = g_{31}$, entailing $\hat{G} = 0$, the integral in the right-hand side of (B.17) is of elliptic type (of course the same outcome, namely the elliptic character of the solutions [9], characterizes any case with two equal coupling constants, although this is not immediately evident from (B.17)). But not much enlightenment seems to obtain, even in this (somewhat simpler) case, from an attempt to perform explicitly the integration in the right-hand side of (B.17).

One must rather try and evince information directly from the integral representation of $F(\theta)$, see (B.12b) with (B.8b), or (B.17), or from the following representation which the diligent reader will have no difficulty in deriving:

$$F(\theta) = (2i)^{-1} \int_{\exp(2i\theta)}^{\infty} dw w^{-1} w^3 - 1 [w(\theta)]^{1/2}; \quad (\text{B.19a})$$

$$w(\theta) = w^3 - 1 - 4(AD)^2 w^{-1} g_{12} [w - \exp(2i\theta)]^2 [w - \exp(-2i\theta)]^2 + (w-1)^2 g_{23} [w - \exp(-2i\theta)]^2 + g_{31} [w - \exp(2i\theta)]^2; \quad (\text{B.19b})$$

It is now clear from these formulas, together with (B.7), (B.10) and (B.12b), that | just as in the integrable equal-coupling-constants case | also in the case with arbitrary coupling constants the solutions $z_n(t)$ feature two kinds of square-root branch points: those associated with triple collisions, which occur at $t = t_{ij}$, see (B.10b), (B.10d), and those associated with the vanishing of the derivative $F^0(t) = dF(t)/dt$ of $F(t)$, namely those associated with the 3 values $b_1 = 0$, $b_2 = 2 = 3$, $b_3 = 2 = 3$ (see (B.19); of course b_i is defined mod 2), see (B.6b)), which of course correspond, as expected, to pair collisions, see (B.7). It is however not possible now | in contrast to the integrable case, see (B.15) | to obtain an explicit expression for the values b_i of t at which these branch points occur: but we infer from (B.17) and (B.12a) that generally there is an infinite number of such branch points in the complex t -plane (again, in contrast to the integrable case, when there only are three, see (B.15)). It is on the other hand easy to obtain from these formulas an explicit expression for the behavior of $z_n(t)$ for $t \rightarrow t_{ij}$, for instance for the branch point with $b_1(t_{ij}) = 0$,

$$z_n(t) = [(b_1(t_{ij}) - A)^{1/2} + O((t - t_{ij})^{1/2})]; \quad (\text{B } 20a)$$

$$= i(b_{12}=2)^{1/4} D^{1/2} + (b_1 + B)^{1/2}; \quad (\text{B } 20b)$$

References

- [1] Calogero F, Periodic Solutions of a System of Complex ODEs, Phys. Lett. A 293 (2002), 146{150.
- [2] Calogero F, Many-Body Problems Amenable to Exact Treatments, Springer Lecture Notes in Physics Monograph, Volume 66, 2001.
- [3] Calogero F and Francoise J-P, Periodic Motions Galore: How to Modify Nonlinear Evolution Equations So That They Feature a Lot of Periodic Solutions, J. Nonlin. Math. Phys. 9 (2002), 99{125.
- [4] Calogero F, Differential Equations Featuring Many Periodic Solutions, in: Geometry and Integrability, Edited by L Mason and Y Nutku, London Mathematical Society Lecture Notes Vol. 295, Cambridge University Press (in press).
- [5] Calogero F, Francoise J-P and Sommacal M, Periodic Solutions of a Many-Rotator Problem in the Plane. II. Analysis of Various Motion, J. Nonlin. Math. Phys. (in press).
- [6] Sommacal M, Studio con tecniche numeriche ed analitiche di problemi a molti corpi nel piano, Dissertation for the "Laurea in Fisica", Department of Physics, University of Rome "La Sapienza", 2002.
- [7] Sommacal M, A Property of the Calogero-Moser System, Phys. Lett. A (submitted to).
- [8] Calogero F, The "Neatest" Many-Body Problem Amenable to Exact Treatments (a "Gold-sh"?), Physica D 152{153 (2001), 78{84.
- [9] Calogero F, Three Solvable Many-Body Problems in the Plane, Acta Applicandae Mathematicae 51 (1998), 93{111.
- [10] Jacobi C, Problem a trium corporum mutuis attractionibus cubis distantiarum inverse proportionalibus recta linea semoventium, in Gesammelte Werke, Vol. 4, Berlin, 1866, 533{539.

-
- [11] Khandekar D C and Lawande S V, Solution of a One-Dimensional Three-Body Problem in Classical Mechanics, Amer. J. Phys. 40 (1972), 458{462.